Double parton scattering and double parton distributions.

overview and recent developments

January 10, 2023

P. Plößl [1]

[1]Deutsches Elektronen-Synchrotron DESY

Part I

A brief introduction to double parton scattering.

What is double parton scattering?

Double parton scattering (DPS) describes two individual hard interactions in a single hadron-hadron collision:

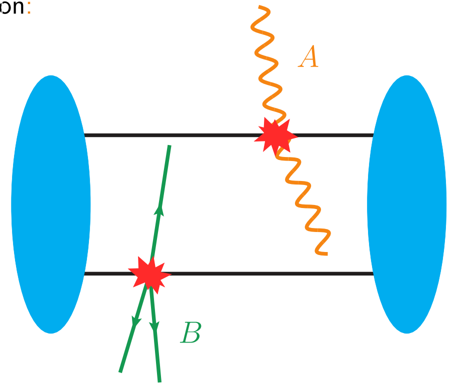

- Already observed at previous colliders at CERN and at the Tevatron.
- More data available from the LHC and more to come from HL-LHC.

DPS is naturally associated with the situation where the final state can be separated into two subsets with individual hard scales.

When is DPS relevant and why is it interesting?

- Whilst generally suppressed compared to single parton scattering (SPS), DPS may be enhanced for final states with small transverse momenta or large separation in rapidity.

- When production of final states via SPS involves small coupling constants or higher orders, DPS may give leading contributions (like-sign W production):

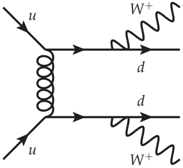

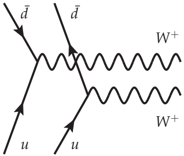

$\longrightarrow$ background to the search for new physics with like-sign lepton pairs.

- Relative importance of DPS increases with collision energy ($\sigma_{\text{DPS}} \sim \text{PDF}^4$ vs. $\sigma_{\text{SPS}} \sim \text{PDF}^2$).

- DPS gives access to information about hadron structure not accessible in other processes: spatial, spin, and colour correlations between two partons.

Experimental observations of DPS: Overview.

DPS has been observed in a broad class of processes already:

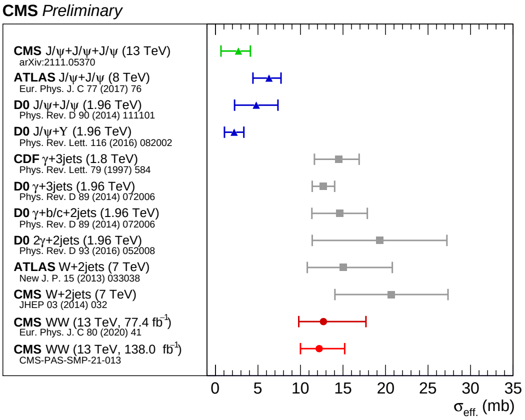

- The effective cross section σ_{eff} is a measure for the relative importance of DPS compared to SPS.
- Should be process independent if partons inside the proton were completely uncorrelated.
- Tension between effective cross sections for gluon and quark initiated processes.

⟶ Will come back to this in a moment!

Experimental observations of DPS: Same-sign W.

Same-sign W pair production is one of the theoretically cleanest DPS channels and has recently been measured by the CMS collaboration:

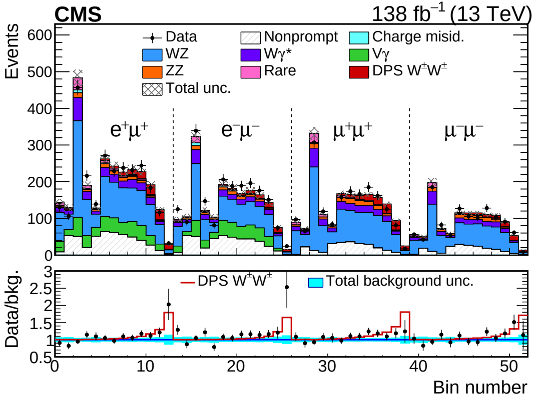

[CMS-PAS-SMP-21-013]

Part II

Double parton scattering theory.

Development of a theory framework for DPS.

Work towards a theoretical description of DPS started already in the 80's:

LO factorisation formula based on a parton model picture [Politzer, 1980; Paver and Treleani, 1982; Mekhfi, 1985]

$$\sigma^{\mathsf{DPS}}_{A,B} = \hat{\sigma}_{ik\to A}(x_1\bar{x}_1 s)\,\hat{\sigma}_{jl\to B}(x_2\bar{x}_2 s)\int \mathrm{d}^2\boldsymbol{y}\,F_{ij}(x_1,x_2,\boldsymbol{y})\,F_{kl}(\bar{x}_1,\bar{x}_2,\boldsymbol{y})$$

The LHC era has seen increasing interest in DPS: Development of a full QCD description!

- Systematic QCD description. [Blok et al., 2011; Diehl et al., 2011; Manohar and Waalewijn, 2012; Ryskin and Snigirev, 2012]
- Factorization proof for double DY. [Diehl, Gaunt, Ostermeier, Plößl, Schäfer, 2015; Diehl and Nagar, 2019]
- Disentangling SPS and DPS. [Gaunt and Stirling, 2011; Diehl, Gaunt and Schönwald, 2017]

Development of a theory framework for DPS.

Work towards a theoretical description of DPS started already in the 80's:

LO factorisation formula based on a parton model picture [Politzer, 1980; Paver and Treleani, 1982; Mekhfi, 1985]

$$\sigma^{\mathsf{DPS}}_{A,B} = \hat{\sigma}_{ik\to A}(x_1\bar{x}_1 s)\,\hat{\sigma}_{jl\to B}(x_2\bar{x}_2 s)\int \mathrm{d}^2\boldsymbol{y}\, F_{ij}(x_1, x_2, \boldsymbol{y})\, F_{kl}(\bar{x}_1, \bar{x}_2, \boldsymbol{y})$$

The LHC era has seen increasing interest in DPS: Development of a full QCD description!

- Systematic QCD description. [Blok et al., 2011; Diehl et al., 2011; Manohar and Waalewijn, 2012; Ryskin and Snigirev, 2012]
- Factorization proof for double DY. [Diehl, Gaunt, Ostermeier, Plößl, Schäfer, 2015; Diehl and Nagar, 2019]
- Disentangling SPS and DPS. [Gaunt and Stirling, 2011; Diehl, Gaunt and Schönwald, 2017]

Development of a theory framework for DPS.

Work towards a theoretical description of DPS started already in the 80's:

LO factorisation formula based on a parton model picture [Politzer, 1980; Paver and Treleani, 1982; Mekhfi, 1985]

$$\sigma^{\text{DPS}}_{A,B} = \hat{\sigma}_{ik\to A}(x_1\bar{x}_1 s)\,\hat{\sigma}_{jl\to B}(x_2\bar{x}_2 s)\int \mathrm{d}^2\boldsymbol{y}\,F_{ij}(x_1,x_2,\boldsymbol{y})\,F_{kl}(\bar{x}_1,\bar{x}_2,\boldsymbol{y})$$

The LHC era has seen increasing interest in DPS: Development of a full QCD description!

- Systematic QCD description. [Blok et al., 2011; Diehl et al., 2011; Manohar and Waalewijn, 2012; Ryskin and Snigirev, 2012]
- Factorization proof for double DY. [Diehl, Gaunt, Ostermeier, Plößl, Schäfer, 2015; Diehl and Nagar, 2019]
- Disentangling SPS and DPS. [Gaunt and Stirling, 2011; Diehl, Gaunt and Schönwald, 2017]

Factorization for DPS: The double Drell-Yan process.

The general procedure towards a factorization proof for DPS is the same as in the SPS case:

- Identification of leading momentum regions and subgraphs (hard, collinear, soft) using the method by Libby and Sterman.
- Kinematic approximation of soft and collinear gluon momenta.
- Decoupling of collinear gluons.
- Proof that the Glauber momentum region can be avoided. [Diehl, Gaunt, Ostermeier, Plößl, Schäfer, 2015]
- Decoupling of soft gluons. [Diehl and Nagar, 2019]
- Handling of rapidity and UV divergences.

Factorization for double Drell-Yan has been proven at the same level of rigor as in the SPS case!

Leading regions for the double Drell-Yan process.

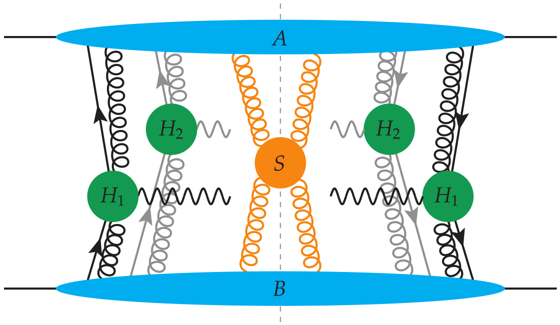

- Two hard subgraphs (H_1 and H_2) on either side of the final state cut.
- One collinear subgraph (A and B) for each colliding proton.
- A soft subgraph (S).
- An arbitrary number of soft and collinear gluons connecting the soft and hard subgraphs to the collinear subgraph, respectively.

Factorization for DPS: The double Drell-Yan process.

The general procedure towards a factorization proof for DPS is the same as in the SPS case:

- Identification of leading momentum regions and subgraphs (hard, collinear, soft) using the method by Libby and Sterman.
- Kinematic approximation of soft and collinear gluon momenta.
- Decoupling of collinear gluons.
- Proof that the Glauber momentum region can be avoided. [Diehl, Gaunt, Ostermeier, Plößl, Schäfer, 2015]
- Decoupling of soft gluons. [Diehl and Nagar, 2019]
- Handling of rapidity and UV divergences.

Factorization for double Drell-Yan has been proven at the same level of rigor as in the SPS case!

Factorized cross section for the double Drell-Yan process.

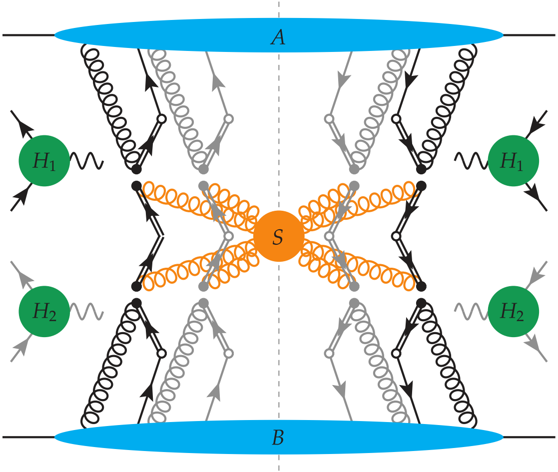

- Collinear gluons have been absorbed into collinear matrix elements (to be identified as double parton distributions), acting as gauge links.
- Soft gluons have been absorbed into the soft factor, a matrix element of Wilson line operators.
- Hard subgraphs are reduced to parton level cross sections that can be calculated in perturbation theory.

SPS-DPS double counting: Issue.

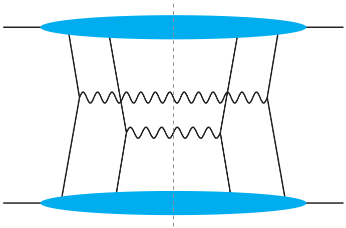

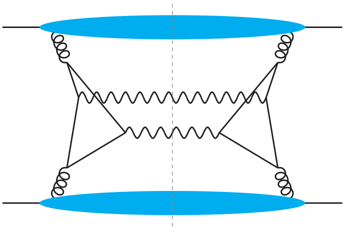

Should the process on the right be considered as a DPS process or as a loop correction to SPS?

- Both: SPS for large transverse momenta (small $\boldsymbol{y}$), DPS for small transverse momenta (large $\boldsymbol{y}$).
- Solution: Diehl-Gaunt-Schönwald subtraction formalism. [Diehl, Gaunt and Schönwald, 2017]

$\longrightarrow$ Use that for small distances $\boldsymbol{y}$ the DPDs can be calculated in perturbation theory ($\boldsymbol{y}^{-2}$ behaviour)!

SPS-DPS double counting: Issue.

Should the process on the right be considered as a DPS process or as a loop correction to SPS?

- Both: SPS for large transverse momenta (small y), DPS for small transverse momenta (large y).
- Solution: Diehl-Gaunt-Schönwald subtraction formalism. [Diehl, Gaunt and Schönwald, 2017]

$\longrightarrow$ Use that for small distances y the DPDs can be calculated in perturbation theory (y^{-2} behaviour)!

SPS-DPS double counting: Issue.

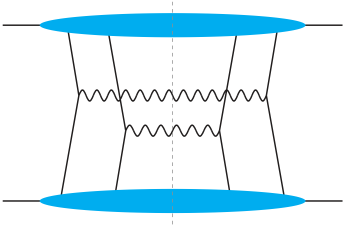

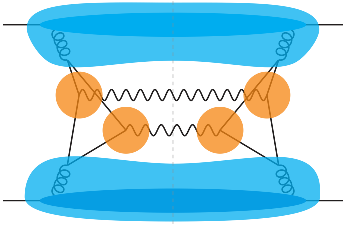

Should the process on the right be considered as a DPS process or as a loop correction to SPS?

- Both: SPS for large transverse momenta (small $\boldsymbol{y}$), DPS for small transverse momenta (large $\boldsymbol{y}$).
- Solution: Diehl-Gaunt-Schönwald subtraction formalism. [Diehl, Gaunt and Schönwald, 2017]

$\longrightarrow$ Use that for small distances $\boldsymbol{y}$ the DPDs can be calculated in perturbation theory ($\boldsymbol{y}^{-2}$ behaviour)!

SPS-DPS double counting: Solution.

Two issues with SPS+DPS cross sections: SPS-DPS double counting and the DPS splitting singularity.

Defining the DPS cross section with a lower cut-off regulates the splitting singularity:

$$\sigma^{\text{DPS}}_{A,B} = \hat{\sigma}_{ik\to A}(x_1\bar{x}_1 s)\,\hat{\sigma}_{jl\to B}(x_2\bar{x}_2 s)\int d^2\boldsymbol{y}\,\Phi^2(y\nu)F_{ij}(x_1,x_2,\boldsymbol{y})\,F_{kl}(\bar{x}_1,\bar{x}_2,\boldsymbol{y})$$

with

$$\Phi(u)\to 0 \qquad \text{for } u\to 0\,,$$

$$\Phi(u)\to 1 \qquad \text{for } u\gg 1\,.$$

The double counting issue is then solved by a subtraction term:

$$\sigma^{\text{tot}}_{A,B} = \sigma^{\text{SPS}}_{A,B} + \sigma^{\text{DPS}}_{A,B} - \sigma^{\text{sub}}_{A,B}\,.$$

SPS-DPS double counting: Calculating the subtraction term.

Consider the LO example:

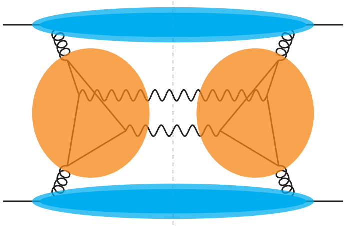

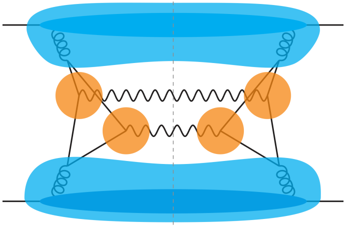

Double counting due to perturbative splitting contributions in SPS and DPS cross sections.

Subtraction term given by:

$$\sigma^{\text{sub}}_{A,B} = \hat{\sigma}_{ik\to A}(x_1\bar{x}_1 s)\,\hat{\sigma}_{jl\to B}(x_2\bar{x}_2 s)\int \mathrm{d}^2\boldsymbol{y}\,\Phi^2(y\nu)F^{\text{split}}_{ij}(x_1,x_2,\boldsymbol{y})\,F^{\text{split}}_{kl}(\bar{x}_1,\bar{x}_2,\boldsymbol{y})$$

where F^{split} is the perturbative small $\boldsymbol{y}$ expression for the DPDs.

SPS-DPS double counting: Subtraction at work.

Consider how the subtraction works for the LO example:

$$\sigma_{A,B}^{\text{tot}} = \sigma_{A,B}^{\text{SPS}} + \sigma_{A,B}^{\text{DPS}} - \sigma_{A,B}^{\text{sub}} .$$

Small y: For small y ($\mathcal{O}(1/Q)$) one finds that $F \simeq F^{\text{split}}$ and thus

$$\sigma_{A,B}^{\text{DPS}} \simeq \sigma_{A,B}^{\text{sub}} \qquad \sigma_{A,B}^{\text{tot}} \simeq \sigma_{A,B}^{\text{SPS}}$$

Large y: For large y ($\gg \mathcal{O}(1/Q)$) the leading contribution to the SPS cross section is the splitting contribution in the DPS region such that

$$\sigma_{A,B}^{\text{SPS}} \simeq \sigma_{A,B}^{\text{sub}} \qquad \sigma_{A,B}^{\text{tot}} \simeq \sigma_{A,B}^{\text{DPS}}$$

$\longrightarrow$ The DGS subtraction formalism consistently solves the SPS-DPS double counting issue.

Approximation of DPS cross section: DPS pocket formula.

A widely used approximation in phenomenological studies of DPS is the following:

$$F_{ij}(x_1, x_2, \boldsymbol{y}) = f_i(x_1)\, f_j(x_2)\, g(\boldsymbol{y})$$

yielding a simplified expression for the DPS factorization formula (“DPS pocket formula”):

$$\sigma^{DPS}_{A,B} = \frac{\sigma^{SPS}_{A}\, \sigma^{SPS}_{B}}{\sigma_{\text{eff}}}$$

where the “effective” cross section is given by

$$\sigma^{-1}_{\text{eff}} = \int \mathrm{d}^2\boldsymbol{y}\, \big(g(\boldsymbol{y})\big)^2$$

and should be process-independent if the approximations were justified!

Part III

Definitions and properties of DPDs.

Position and momentum assignments in DPDs and dTMDs.

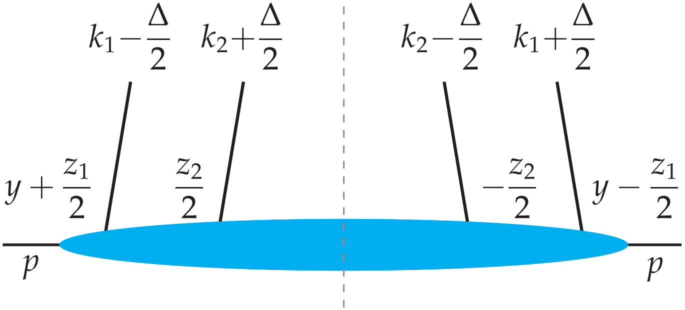

with Fourier conjugate positions and momenta $z_1 \leftrightarrow k_1$, $z_2 \leftrightarrow k_2$, and $y \leftrightarrow \Delta$.

Definition of DPDs.

Bare unsubtracted position space DPDs:

$$F_{B\,\mathrm{us},a_1 a_2}^{r_1 r_1' \, r_2 r_2'}(x_i, \boldsymbol{y}) = (x_1 p^+)^{-n_1} \, (x_2 p^+)^{-n_2} \; 2p^+ \int \mathrm{d}y^- \left[\prod_{i=1}^{2} \int \frac{\mathrm{d}z_i^-}{2\pi} \, e^{i x_i z_i^- p^+} \right] \times \langle p | \, \mathcal{O}_{a_1}^{r_1 r_1'}(y, z_1) \, \mathcal{O}_{a_2}^{r_2 r_2'}(0, z_2) \, | p \rangle \Big|_{y^+=0, \boldsymbol{z}_i=0}$$

where $n_i = 0$ for quarks and $n_i = 1$ for gluons and the twist-2 operators are defined in terms of quark- and gluon-fields and Wilson lines as:

$$\mathcal{O}_a^{ii'}(y,z) = \bar{q}_{j'}(\xi_-) \left[W^\dagger(\xi_-, v_L) \right]_{j'i'} \Gamma_a \left[W(\xi_+, v_L) \right]_{ij} q_j(\xi_+) \qquad \text{for quarks} \,,$$

$$\mathcal{O}_a^{aa'}(y,z) = \left[G^{+k'}(\xi_-) \right]^{b'} \left[W^\dagger(\xi_-, v_L) \right]^{b'a'} \Pi_a^{kk'} \left[W(\xi_+, v_L) \right]^{ab} \left[G^{+k}(\xi_+) \right]^{b} \qquad \text{for gluons} \,,$$

with $\xi_\pm = y \pm z/2$, $z^+ = 0$ and where Γ_a and Π_a project onto different definite polarisation states.

Definition of the DPS soft factors.

Bare position space DPS soft factor:

$$\left[S_{B,a_1a_2}(\boldsymbol{y}; v_L, v_R)\right]^{r_1 r_1' r_2 r_2'}_{s_1 s_1' s_2 s_2'} = \left\langle 0 \,\middle|\, \left[O_S(\boldsymbol{y}, \boldsymbol{0}; v_L, v_R)\right]^{r_1 r_1', s_1 s_1'} \left[O_S(\boldsymbol{0}, \boldsymbol{0}; v_L, v_R)\right]^{r_2 r_2', s_2 s_2'} \,\middle|\, 0 \right\rangle$$

where the colour indices r_i are in the fundamental or adjoint representation if a_i is a quark or gluon, respectively, and:

$$\left[O_S(\boldsymbol{y}, \boldsymbol{z}; v_L, v_R)\right]^{rr', ss'} = \left[W(\boldsymbol{y} + \tfrac{1}{2}\boldsymbol{z}, v_L)\, W^\dagger(\boldsymbol{y} + \tfrac{1}{2}\boldsymbol{z}, v_R)\right]_{rs} \left[W(\boldsymbol{y} - \tfrac{1}{2}\boldsymbol{z}, v_R)\, W^\dagger(\boldsymbol{y} - \tfrac{1}{2}\boldsymbol{z}, v_L)\right]_{s'r'}$$

The soft factor defined above is for the production of colour singlet states.

Spin structure of DPDs.

DPDs exhibit a rich spin structure, giving access to spin correlations between two partons inside a proton.

The Γ and Π matrices projecting on definite quark and gluon polarizations are given by:

$$\Gamma_q = \frac{\gamma^+}{2}\,, \qquad \Gamma_{\Delta q} = \frac{\gamma^+\gamma_5}{2}\,, \qquad \Gamma^j_{\delta q} = \frac{\sigma^{+j}}{2}$$

$$\Pi_g^{kk'} = \delta^{kk'}\,, \qquad \Pi_{\Delta g}^{kk'} = i\,\varepsilon^{kk'}\,, \qquad \Pi_{\delta g}^{kk'jj'} = \tau^{kk',jj'}$$

for unpolarized, longitudinally polarized, and transversally/linearly polarized quarks and gluons, respectively.

In the TMD case all possible combinations of quark and gluon polarizations are admissible, whereas in the collinear DPD case considered here some - like $q\Delta q$ - are identical to zero (similar to TMD vs. PDF).

Colour structure of DPDs.

Compared to PDFs, DPDs have a more complex colour structure, as now four parton legs have to be coupled to an overall colour singlet. This can be made more systematic by:

- coupling the colour indices r_i and r_i' pairwise to irreducible representations R_i of $SU(N)$ such that $R_1 R_2$ form an overall colour singlet:

$$ {}^{R_1 R_2}F_{B\,\mathrm{us},a_1 a_2} \sim P_{\overline{R}_1 \overline{R}_2} F_{B\,\mathrm{us},a_1 a_2} $$

- decomposing the full colour structure in terms of these combinations:

$$ F_{B\,\mathrm{us},a_1 a_2} \sim \sum_{R_1, R_2} P_{R_1 R_2}\, {}^{R_1 R_2}F_{B\,\mathrm{us},a_1 a_2} $$

In addition to $R_1 R_2 = 1\,1$ one finds the following colour non-singlet channels:

- $R_1 R_2 = 8\,8$ for $a_1 a_2 = q q'$.
- $R_1 R_2 = 8\,A$ and $8\,S$ for $a_1 a_2 = q g$.
- $R_1 R_2 = A\,A$, $S\,S$, $A\,S$, $S\,A$, $10\,\overline{10}$, $\overline{10}\,10$ and $27\,27$ for $a_1 a_2 = g g$.

Colour structure of the DPS soft factor.

Much in the same way as DPDs, the colour structure of the DPS soft factor can be decomposed as:

$$S_{B,a_1a_2} \sim \sum_{\substack{R_1R_2\\R_1'R_2'}} P_{R_1R_2} P_{R_1'R_2'} \, {}^{R_1R_2}_{R_1'R_2'}S_{B,a_1a_2}$$

with

$$\boxed{{}^{R_1R_2}_{R_1'R_2'}S_{B,a_1a_2} \sim P_{\overline{R}_1\overline{R}_2} S_{B,a_1a_2} P_{\overline{R}_1'\overline{R}_2'}}$$

For the collinear DPS soft factor the colour structure simplifies:

$${}^{R_1R_2}_{R_1'R_2'}S_{B,a_1a_2} = \delta_{R_1\overline{R}_1'}\delta_{R_2\overline{R}_2'} \, {}^{R_1R_2}_{\overline{R}_1\overline{R}_2}S_{B,a_1a_2} \equiv \delta_{R_1\overline{R}_1'}\delta_{R_2\overline{R}_2'} \, {}^{R_1R_2}S_{B,a_1a_2}$$

Absorbing the soft factor into DPDs.

DPDs contain rapidity divergences associated with light-like Wilson lines.

These cancel in the complete factorized cross section against rapidity divergences in the soft factor.

Solution: Absorbing the soft factor into the DPDs, defining rapidity finite distributions!

$$^{R_1R_2}F_{B,a_1a_2}(x_i, y, \zeta_p) = \lim_{\rho\to\infty} \frac{^{R_1R_2}F_{B\,\text{us},a_1a_2}(x_i, y, \rho)}{\sqrt{^{R_1R_2}S_{B,a_1a_2}(y, \rho, \zeta_p)}}$$

DPS analog for TMD subtraction [Collins, 2011].

where the limit $\rho \to \infty$ corresponds to removing the rapidity regulator.

Note: Definition of ζ_p differs from the one of ζ for TMDs:

$$\zeta_p \zeta_{\bar{p}} = (2p^+\bar{p}^-)^2 = s^2 \qquad \text{vs.} \qquad \zeta\bar{\zeta} = x^2\bar{x}^2(2p^+\bar{p}^-)^2 = Q^4$$

UV renormalisation and scale dependence of DPDs.

For DPDs one has in addition to UV divergences associated with vertex and self-energy corrections of composite operators at vanishing transverse separation also UV divergences associated with ladder graphs, as two quark or gluon fields can sit at the same transverse position. These are renormalised via:

$$ {}^{R_1R_2}F_{a_1a_2}(x_i, y, \zeta_p, \mu_i) = \left[\sum_{R_1' R_2'} {}^{R_1\overline{R}_1'}Z_{a_1b_1}(\mu_1, x_1^2\zeta_p) \underset{1}{\otimes} {}^{R_2\overline{R}_2'}Z_{a_2b_2}(\mu_2, x_2^2\zeta_p) \underset{2}{\otimes} {}^{R_1' R_2'}F_{B,b_1b_2}(y, \zeta_p) \right](x_i) $$

with:

$$ \frac{d}{d\log\mu}\, {}^{RR''}Z_{ab}(\mu) = 2\sum_{R'} {}^{R\overline{R}'}P_{ac}(\mu) \otimes {}^{R'R''}Z_{cb}(\mu) $$

resulting in the DGLAP scale dependence of DPDs:

$$ \boxed{\frac{\partial}{\partial\log\mu_1}\, {}^{R_1R_2}F_{a_1a_2}(x_i, y, \zeta_p, \mu_i) = 2\left[\sum_{R_1'} {}^{R_1\overline{R}_1'}P_{a_1b_1}(\mu) \underset{1}{\otimes} {}^{R_1' R_2}F_{b_1a_2}(y, \zeta_p, \mu_i) \right](x_i)} $$

Rapidity evolution of DPDs.

As a result of splitting the soft factor into two parts and absorbing these into the DPDs, the distributions acquire a dependence on the rapidity parameter ζ_p, governed by a Collins-Soper type equation:

$$\frac{\partial}{\partial \log \zeta_p} {}^{R_1 R_2}F(x_i, \boldsymbol{y}, \zeta_p, \mu_i) = \frac{1}{2} {}^{R_1}J(\boldsymbol{y}, \mu_i) \, {}^{R_1 R_2}F(x_i, \boldsymbol{y}, \zeta_p, \mu_i)$$

where the scale dependence of the Collins-Soper kernels is given by:

$$\frac{\partial}{\partial \log \mu_1} {}^{R}J(\boldsymbol{y}, \mu_i) = -\gamma_J^R(\mu_1)$$

Part IV

DPDs in the limit of small interparton distance y.

Perturbative splitting in DPDs.

In the limit of small distance $\boldsymbol{y}$ the leading contribution to a DPD is due to the perturbative splitting of one parton into two and can be calculated in perturbation theory:

$$ {}^{R_1R_2}F_{a_1a_2}(x_i, y, \zeta_p, \mu) \overset{\boldsymbol{y}\to 0}{=} \frac{1}{\pi y^2} \left[{}^{R_1R_2}V_{a_1a_2,a_0}(y, \zeta_p, \mu) \underset{12}{\otimes} f_{a_0}(\mu) \right] (x_i $$

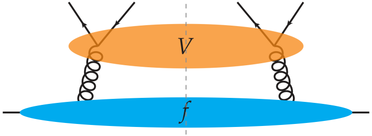

At LO the convolution reduces to a simple product:

$$ {}^{R_1R_2}F^{(1)}_{a_1a_2}(x_i, y, \zeta_p, \mu) \overset{\boldsymbol{y}\to 0}{=} \frac{a_s}{\pi y^2} \, {}^{R_1R_2}V^{(1)}_{a_1a_2,a_0} \left(\frac{x_1}{x_1+x_2} \right) \frac{f_{a_0}(x_1+x_2\mu)}{x_1+x_2} $$

with

$$ {}^{R_1R_2}V^{(1)}_{gg,g}(z) = c_{gg,g}(R_1R_2) \, 2\, C_A \left(\frac{\bar{z}}{z} + \frac{z}{\bar{z}} + z\bar{z} \right) $$

Perturbative splitting in DPDs.

In the limit of small distance $\boldsymbol{y}$ the leading contribution to a DPD is due to the perturbative splitting of one parton into two and can be calculated in perturbation theory:

$$^{R_1R_2}F_{a_1a_2}(x_i, y, \zeta_p, \mu) \overset{\boldsymbol{y}\to 0}{=} \frac{1}{\pi y^2} \left[{}^{R_1R_2}V_{a_1a_2,a_0}(y, \zeta_p, \mu) \underset{12}{\otimes} f_{a_0}(\mu) \right](x_i)$$

formally OPE of $\mathcal{O}(y, z_1)\mathcal{O}(0, z_2)$ for $y \to 0$

At LO the convolution reduces to a simple product:

$$^{R_1R_2}F^{(1)}_{a_1a_2}(x_i, y, \zeta_p, \mu) \overset{\boldsymbol{y}\to 0}{=} \frac{a_s}{\pi y^2} \, {}^{R_1R_2}V^{(1)}_{a_1a_2,a_0}\left(\frac{x_1}{x_1+x_2}\right) \frac{f_{a_0}(x_1+x_2\mu)}{x_1+x_2}$$

with

$$^{R_1R_2}V^{(1)}_{gg,g}(z) = c_{gg,g}(R_1R_2)\, 2\, C_A \left(\frac{\bar{z}}{z} + \frac{z}{\bar{z}} + z\bar{z}\right)$$

Perturbative splitting in DPDs.

In the limit of small distance $\boldsymbol{y}$ the leading contribution to a DPD is due to the perturbative splitting of one parton into two and can be calculated in perturbation theory:

$$^{R_1R_2}F_{a_1a_2}(x_i, y, \zeta_p, \mu) \overset{\boldsymbol{y}\to 0}{=} \frac{1}{\pi y^2} \left[{}^{R_1R_2}V_{a_1a_2,a_0}(y, \zeta_p, \mu) \underset{12}{\otimes} f_{a_0}(\mu) \right](x_i)$$

formally OPE of $\mathcal{O}(y, z_1)\mathcal{O}(0, z_2)$ for $y \to 0$

At LO the convolution reduces to a simple product:

$$^{R_1R_2}F^{(1)}_{a_1a_2}(x_i, y, \zeta_p, \mu) \overset{\boldsymbol{y}\to 0}{=} \frac{a_s}{\pi y^2} \, {}^{R_1R_2}V^{(1)}_{a_1a_2,a_0}\left(\frac{x_1}{x_1 + x_2}\right) \frac{f_{a_0}(x_1 + x_2\mu)}{x_1 + x_2}$$

with

$$^{R_1R_2}V^{(1)}_{q\bar{q},g}(z) = c_{q\bar{q},g}(R_1R_2)\, T_F \left(z^2 + \bar{z}^2\right)$$

Perturbative splitting in DPDs.

In the limit of small distance $\boldsymbol{y}$ the leading contribution to a DPD is due to the perturbative splitting of one parton into two and can be calculated in perturbation theory:

$$ {}^{R_1R_2}F_{a_1a_2}(x_i, y, \zeta_p, \mu) \overset{\boldsymbol{y}\to 0}{=} \frac{1}{\pi y^2} \left[{}^{R_1R_2}V_{a_1a_2,a_0}(y, \zeta_p, \mu) \underset{12}{\otimes} f_{a_0}(\mu) \right] (x_i) $$

formally OPE of $\mathcal{O}(y, z_1)\mathcal{O}(0, z_2)$ for $y \to 0$

At LO the convolution reduces to a simple product:

$$ {}^{R_1R_2}F^{(1)}_{a_1a_2}(x_i, y, \zeta_p, \mu) \overset{\boldsymbol{y}\to 0}{=} \frac{a_s}{\pi y^2} \, {}^{R_1R_2}V^{(1)}_{a_1a_2,a_0} \left(\frac{x_1}{x_1 + x_2} \right) \frac{f_{a_0}(x_1 + x_2\mu)}{x_1 + x_2} $$

with

$$ {}^{R_1R_2}V^{(1)}_{qg,q}(z) = c_{qg,q}(R_1R_2)\, C_F \,\frac{1+z}{\bar{z}} $$

The "splitting scale".

At which scale μ_{split} should the splitting be evaluated?

The natural scale of the splitting is set by the interparton distance y of the observed partons:

$$\mu_{\text{split}}(y) \sim \frac{1}{y}$$

In order to avoid evaluation of the splitting at non-perturbative scales for large y define:

$$\mu_{\text{split}}(y) = \frac{b_0}{y^*(y)}$$

with

$$y^*(y) = \frac{y}{\sqrt[4]{1 + y^4/y_{\max}^4}}, \qquad y_{\max} = \frac{b_0}{\mu_{\min}}$$

where y^* is adapted from b^* in TMD studies.

Calculating the $1 \to 2$ splitting kernels.

The task of calculating the small distance $1 \to 2$ splitting kernels ${}^{R_1 R_2}V_{a_1 a_2, a_0}$ can be split into the following subtasks:

- Calculation of the bare unsubtracted kernels ${}^{R_1 R_2}V_{B\,\text{us};\, a_1 a_2, a_0}$.
- Cancellation of rapidity divergences.
- Renormalisation of UV divergences.

In the following a brief sketch of each step will be given which will be made more tangible when discussing the computation of the NLO contribution to the kernels.

Bare unsubtracted kernels I.

In order to calculate the bare unsubtracted $1 \to 2$ splitting kernels it is advantageous to work in momentum space where the kernels can be calculated from Feynman diagrams.

Use to this end that the position and momentum space DPDs are related by:

$$^{R_1 R_2}F_{B\,\text{us};\,a_1 a_2}(x_i, y, \rho) = \int \frac{\mathrm{d}^{2-2\varepsilon}\boldsymbol{\Delta}}{(2\pi)^{2-2\varepsilon}} e^{-i\boldsymbol{\Delta y}}\, {}^{R_1 R_2}F_{B\,\text{us};\,a_1 a_2}(x_i, \Delta, \rho)$$

For large $\boldsymbol{\Delta}$ the momentum space DPDs can be computed in perturbation theory as:

$$^{R_1 R_2}F_{B\,\text{us};\,a_1 a_2}(x_i, \Delta, \rho) \overset{\boldsymbol{\Delta}\to\infty}{=} \left[{}^{R_1 R_2}W_{B\,\text{us};\,a_1 a_2, a_0}(\Delta, \rho) \underset{12}{\otimes} f_{B, a_0} \right](x_i)$$

The position and momentum space kernels are thus related by:

$$\frac{\Gamma(1-\varepsilon)}{(\pi y)^{1-\varepsilon}}\, {}^{R_1 R_2}V_{B\,\text{us};\,a_1 a_2, a_0}(z_i, y, \rho) = \int \frac{\mathrm{d}^{2-2\varepsilon}\boldsymbol{\Delta}}{(2\pi)^{2-2\varepsilon}}\, e^{-i\boldsymbol{\Delta y}}\, {}^{R_1 R_2}W_{B\,\text{us};\,a_1 a_2, a_0}(z_i, \Delta, \rho)$$

Bare unsubtracted kernels II.

The bare unsubtracted momentum space kernels can be obtained from a calculation of the bare unsubtracted momentum space DPD of partons a_1 and a_2 in a parton a_0:

$$^{R_1 R_2}F_{B\,\text{us};\,a_1 a_2/a_0}(x_i, \Delta, \rho) = \sum_{i=0}^{n} \left(\frac{\alpha_s}{2\pi}\right)^i \, {}^{R_1 R_2}F^{(i)}_{B\,\text{us};\,a_1 a_2/a_0}(x_i, \Delta, \rho) + \mathcal{O}\left(\left(\frac{\alpha_s}{2\pi}\right)^{n+1}\right)$$

where

$$^{R_1 R_2}F^{(i)}_{B\,\text{us};\,a_1 a_2/a_0}(x_i, \Delta, \rho) = \sum_b \sum_{j=0}^{i} \left[{}^{R_1 R_2}W^{(i-j)}_{B\,\text{us};\,a_1 a_2, b}(\Delta, \rho) \underset{12}{\otimes} f^{(j)}_{b/a_0} \right](x_i)$$

Note: $f^{(j)}_{b/a}(x) = \delta_{ab}\,\delta(1-x)$ for $j = 0$ and vanishes for $j > 0$.

Bare unsubtracted kernels II.

The bare unsubtracted momentum space kernels can be obtained from a calculation of the bare unsubtracted momentum space DPD of partons a_1 and a_2 in a parton a_0:

$$ {}^{R_1R_2}F_{B\,\mathrm{us};\,a_1a_2/a_0}(x_i,\Delta,\rho) = \sum_{i=0}^{n} \left(\frac{\alpha_s}{2\pi}\right)^i \, {}^{R_1R_2}F^{(i)}_{B\,\mathrm{us};\,a_1a_2/a_0}(x_i,\Delta,\rho) + \mathcal{O}\left(\left(\frac{\alpha_s}{2\pi}\right)^{n+1}\right) $$

where

$$ {}^{R_1R_2}F^{(i)}_{B\,\mathrm{us};\,a_1a_2/a_0}(x_i,\Delta,\rho) = {}^{R_1R_2}W^{(i)}_{B\,\mathrm{us};\,a_1a_2,a_0}(x_i,\Delta,\rho) $$

Note: $f^{(j)}_{b/a}(x) = \delta_{ab}\,\delta(1-x)$ for $j=0$ and vanishes for $j>0$.

Rapidity subtraction and UV renormalisation.

Once the bare unsubtracted position space kernels have been obtained from the momentum space kernels the rapidity subtraction can be performed:

$$ {}^{R_1R_2}V_{B;\,a_1a_2,a_0}(z_i,y,\zeta) = \lim_{\rho\to\infty} \frac{{}^{R_1R_2}V_{B\,\mathrm{us};\,a_1a_2,a_0}(z_i,y,\rho)}{\sqrt{{}^{R_1R_2}S_{B;\,a_1a_2}(z_i,y,\rho,\zeta)}} $$

After this UV renormalisation can be performed, following from the renormalisation prescription of the full position space DPD:

$$ \begin{aligned} &{}^{R_1R_2}V_{a_1a_2,a_0}(z_i,y,z_1z_2\zeta_p,\mu_i) \\ &= \left[\sum_{R_1'R_2'} {}^{R_1\overline{R}_1'}Z_{a_1b_1}(\mu_1,z_1^2\zeta_p) \underset{1}{\otimes} {}^{R_2\overline{R}_2'}Z_{a_2b_2}(\mu_2,z_2^2\zeta_p) \underset{2}{\otimes} {}^{R_1'R_2'}V_{B,b_1b_2}(y,z_1z_2\zeta_p) \underset{12}{\otimes} {}^{11}Z^{-1}(\mu)\right](z_i) \end{aligned} $$

Motivation for the calculation of NLO $1 \to 2$ splitting kernels.

The reason why the NLO contribution to the $1 \to 2$ splitting kernels is interesting is twofold:

- As DPDs are largely unknown the small y behaviour provides a valuable input for the modelling of DPDs.
- The small y splitting DPDs are needed for the calculation of the subtraction term in the SPS-DPS framework of [Diehl, Gaunt, and Schönwald, 2017].

In a fist step ${}^{R_1 R_2}W^{(2)}_{B\,\text{us}}(\Delta, \rho)$ is calculated, from which the renormalized ${}^{R_1 R_2}V^{(2)}$ is then extracted following a RGE analysis.

The calculation is performed for two different rapidity regulators:

- Collins regulator (first application to a two loop calculation). [Collins, 2011]
- δ regulator. [Echevarria, Scimemi and Vladimirov, 2016]

Identical results are obatined in both schemes! [Diehl, Gaunt, Plößl, and Schäfer, 2019; Diehl, Gaunt, and Plößl, 2021]

From Feynman diagrams to bare unsubtracted kernels.

The NLO $a_0 \to a_1 a_2$ kernel $W^{(2)}_{B\,\mathrm{us},a_1a_2,a_0}$ can be obtained by calculating the DPD for partons a_1, a_2 in parton a_0:

$$F^{(2)}_{B\,\mathrm{us},a_1a_2/a_0}(\Delta,\rho) = W^{(2)}_{B\,\mathrm{us},a_1a_2,a_0}(\Delta,\rho)$$

At NLO one finds the following splitting kernels:

- LO channels: $g \to gg$, $g \to q\bar{q}$, and $q \to qg$
- NLO channels: $g \to qg$, $q \to gg$, $q_j \to q_j q_k$, $q_j \to q_j \bar{q}_k$, $q_j \to q_k \bar{q}_k$

Note: Only LO channels exhibit rapidity divergences.

$1 \to 2$ splitting kernels at NLO.

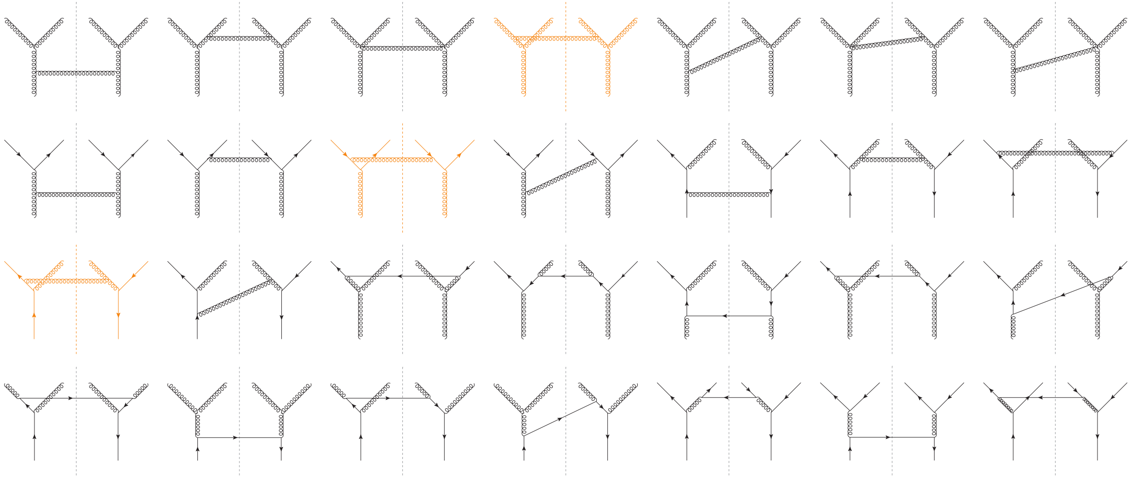

Diagrams in orange give rise to rapidity divergences!

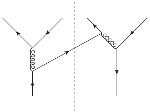

$1 \to 2$ splitting kernels at NLO.

Diagrams in orange give rise to rapidity divergences!

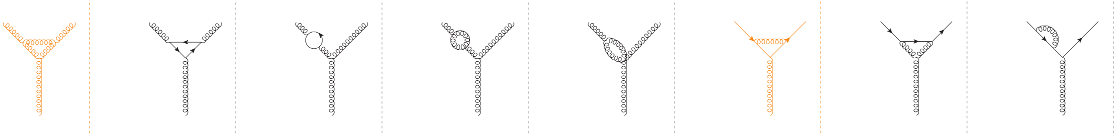

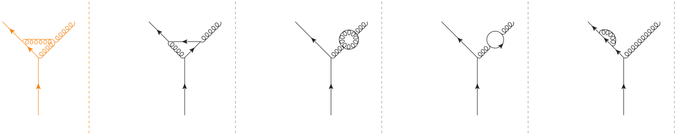

Evaluating real diagrams: Kinematics and minus integrations.

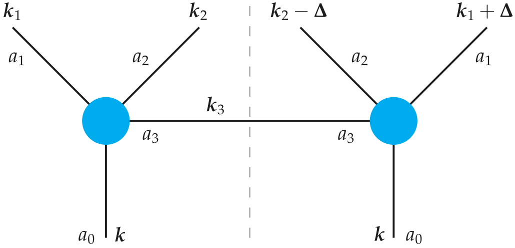

- $k_3 = k - k_1 - k_2$,
- $k_1^+ = z_1 k^+$, $k_2^+ = z_2 k^+$, $\Delta^+ = 0$
- $k_3^+ = z_3 k^+ = (1 - z_1 - z_2) k^+$

$F_{B\,\mathrm{us}}^{(2)}$ and thus $W_{B\,\mathrm{us}}^{(2)}$ is obtained from these diagrams by integrating over k_1^-, k_2^-, Δ^-, $\boldsymbol{k}_1$, and $\boldsymbol{k}_2$:

- The on-shell condition for parton a_3 can be used to perform one of the minus integrations, yielding

$$k_3^- = \frac{\boldsymbol{k}_3^2}{2 z_3 k^+}$$

- For the remaining minus integrations Cauchy's theorem is used.

Evaluating real diagrams: Implementation of rapidity regulators.

Wilson line propagators in the Collins and δ regulator schemes:

$$\lim_{\varepsilon\to 0} \frac{1}{v_L^- k_3^+ + v_L^+ k_3^- + i\varepsilon} + \text{c.c.} = \frac{2}{v_L^- k^+}\, \text{PV}\, \frac{z_3}{z_3^2 - \boldsymbol{k}_3^2 z_1 z_2/\rho} \qquad \text{with} \quad \rho = 2k_1^+ k_2^+ v_L^- / |v_L^+|\,,$$

$$\frac{1}{k_3^+ + i\delta^+} + \text{c.c.} = \frac{2}{k^+} \frac{z_3}{z_3^2 + z_1 z_2/\rho} \qquad \text{with} \quad \rho = k_1^+ k_2^+ / (\delta^+)^2\,.$$

In order to make the rapidity divergences which arise as z_3^{-1} poles for $\rho \to \infty$ explicit (and well defined) the following distributional expansions are performed:

$$\lim_{\rho\to\infty} \text{PV}\, \frac{z_3}{z_3^2 - \boldsymbol{k}_3^2 z_1 z_2/\rho} = \frac{1}{[z_3]_+} + \frac{1}{2}\delta(z_3)\left[\log\frac{\rho}{\boldsymbol{\Delta}^2} - \log(z_1 z_2) - \log\frac{\boldsymbol{k}_3^2}{\boldsymbol{\Delta}^2}\right],$$

$$\lim_{\rho\to\infty} \frac{z_3}{z_3^2 + z_1 z_2/\rho} = \frac{1}{[z_3]_+} + \frac{1}{2}\delta(z_3)\left[\log\rho - \log(z_1 z_2)\right].$$

Evaluating real diagrams: Transverse integrations.

After the rapidity divergences have been regulated the transverse momentum integrations can be performed in both regulator schemes.

To this end the following steps are taken:

- Reduction of the Feynman integrals to master integrals using integration-by-parts relations.
- Computation of the master integrals using the method of differential equations and
  - a transformation to the ε form (also known as Henn's canonical basis),
  - and boundary conditions obtained using the method of regions.

The virtual diagrams can be calculated using the same techniques (and even the same master integrals) as the real ones!

Performing the rapidity subtraction.

As mentioned before a Fourier transform gives the bare unsubtracted NLO position space kernel as:

$$\frac{\Gamma(1-\varepsilon)}{(\pi y^2)^{1-\varepsilon}} \, {}^{R_1 R_2}V^{(2)}_{B\,\mathrm{us}}(y,\rho) = \int \frac{\mathrm{d}^{2-2\varepsilon}\boldsymbol{\Delta}}{(2\pi)^{2-2\varepsilon}} \, e^{-i\boldsymbol{\Delta y}} \, {}^{R_1 R_2}W^{(2)}_{B\,\mathrm{us}}(\Delta,\rho)\,.$$

With this and the definition of the rapidity subtracted DPDs one then gets:

$${}^{R_1 R_2}V^{(2)}_{B}(\zeta_p) = \lim_{\rho\to\infty} \left\{ {}^{R_1 R_2}V^{(2)}_{B\,\mathrm{us}}(\rho) - \frac{1}{2}\, {}^{R_1}S^{(1)}_{B}(\rho,\zeta_p)\, {}^{R_1 R_2}V^{(1)}_{B} \right\},$$

where the involved quantities on the right-hand side generally differ in the two regulator schemes, while the left-hand side is already independent of this choice!

Performing the UV renormalization.

From the renormalization prescription for the DPDs one easily obtains that the renormalized position space splitting kernel is given by:

$$^{R_1R_2}V(y,\mu,x_1x_2\zeta_p) = {}^{R_1\overline{R}_1'}Z(\mu,x_1^2\zeta_p) \underset{1}{\otimes} {}^{R_2\overline{R}_2'}Z(\mu,x_2^2\zeta_p) \underset{2}{\otimes} {}^{R_1'R_2'}V_B(y,\mu,x_1x_2\zeta_p) \underset{12}{\otimes} \left({}^{11}Z\right)^{-1}(\mu)$$

The NLO position space splitting kernel $^{R_1R_2}V^{(2)}$ is then obtained by expanding this relation in α_s and picking the $\mathcal{O}(\alpha_s^2)$ terms:

$$\begin{aligned} &V^{(2)}(y,\mu,\zeta) = \\ &\quad V_{\text{fin}}^{(2)} - \left(\hat{P}^{(0)} \underset{1}{\otimes} \left[V_B^{(1)}\right]_1 + \hat{P}^{(0)} \underset{2}{\otimes} \left[V_B^{(1)}\right]_1 - \left[V_B^{(1)}\right]_1 \underset{12}{\otimes} P^{(0)} + \frac{\beta_0}{2}\left[V_B^{(1)}\right]_1\right) \\ &\quad + \left(L\log\frac{\mu^2}{\zeta} - \frac{L^2}{2} + c_{\overline{\text{MS}}}\right)\frac{\gamma_J^{(0)}}{2}V^{(1)} + L\left(\hat{P}^{(0)} \underset{1}{\otimes} V^{(1)} + \hat{P}^{(0)} \underset{2}{\otimes} V^{(1)} - V^{(1)} \underset{12}{\otimes} P^{(0)} + \frac{\beta_0}{2}V^{(1)}\right) \end{aligned}$$

where $V_{\text{fin}}^{(2)}$ is the finite part of $V_{B\,\text{us}}^{(2)}$, $L = \log\frac{\mu^2 y^2}{b_0^2}$ and $b_0 = 2e^{-\gamma}$.

Analytic structure of results.

NLO position space $1 \to 2$ splitting kernels:

$$
{}^{R_1R_2}V^{(2)}_{a_1a_2,a_0}(z_1,z_2,y,\mu,\zeta) = {}^{R_1R_2}V^{[2,0]}_{a_1a_2,a_0}(z_1,z_2) + L\,{}^{R_1R_2}V^{[2,1]}_{a_1a_2,a_0}(z_1,z_2)
+ \left(L\log\frac{\mu^2}{\zeta} - \frac{L^2}{2}\right)\frac{{}^{R_1}\gamma_J^{(0)}}{2}\,{}^{R_1R_2}V^{(1)}_{a_1a_2,a_0}(z_1,z_2)
$$

where

$$
V^{[2,0]}(z_1,z_2) = V^{[2,0]}_{\text{regular}}(z_1,z_2) + \delta(1-z_1-z_2)\,V^{[2,0]}_{\delta}(z_1,z_2)\,,
$$

$$
V^{[2,1]}(z_1,z_2) = V^{[2,1]}_{\text{regular}}(z_1,z_2) + \frac{1}{[1-z_1-z_2]_+}\,V^{[2,1]}_{+}(z_1,z_2) + \delta(1-z_1-z_2)\,V^{[2,1]}_{\delta}(z_1,z_2)
$$

Small y splitting and massive quarks.

What happens when the scale at which the splitting is evaluated is similar to the mass of a heavy quark?

Should the heavy quark be treated as massless, massive, or absent in the evaluation of the splitting?

Consider and compare in the following two different schemes: [Diehl, Nagar, and Plößl, 2022]

- purely massless scheme:
  - heavy quarks treated as decoupling for $\mu_{\text{split}} \lesssim m_Q$,
  - heavy quarks treated as massless for $\mu_{\text{split}} \gtrsim m_Q$.
- "massive" scheme:
  - heavy quarks treated as decoupling for $\mu_{\text{split}} \ll m_Q$,
  - heavy quarks treated as massive for $\mu_{\text{split}} \sim m_Q$,
  - heavy quarks treated as massless for $\mu_{\text{split}} \gg m_Q$.

Purely massless quarks.

The simplest scheme to handle massive quarks is to treat them as absent below a certain scale and as massless above a certain scale.

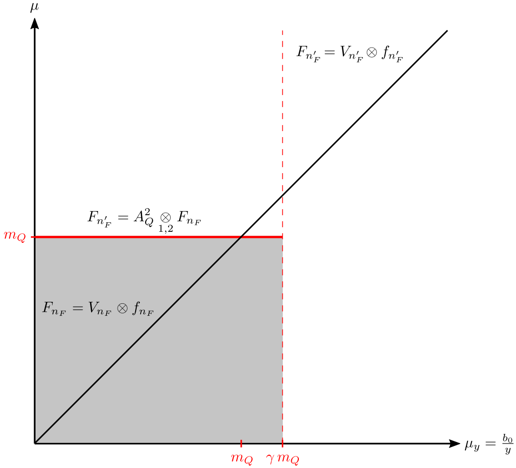

- Below $\mu_y = \gamma\, m_Q$ the DPD is initialized for n_F massless flavours with a n_F flavour PDF.

Purely massless quarks.

The simplest scheme to handle massive quarks is to treat them as absent below a certain scale and as massless above a certain scale.

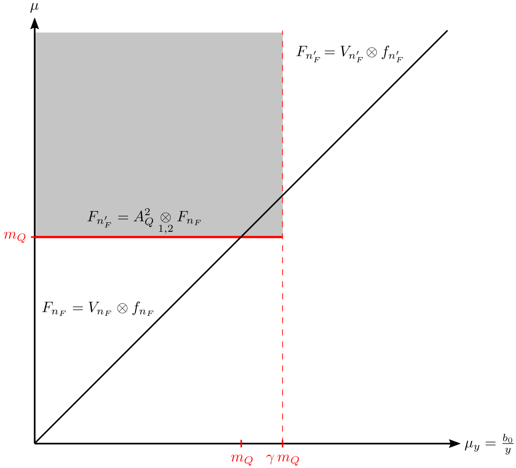

- Below $\mu_y = \gamma\, m_Q$ the $n_F + 1$ DPD is obtained by flavour matching.

Purely massless quarks.

The simplest scheme to handle massive quarks is to treat them as absent below a certain scale and as massless above a certain scale.

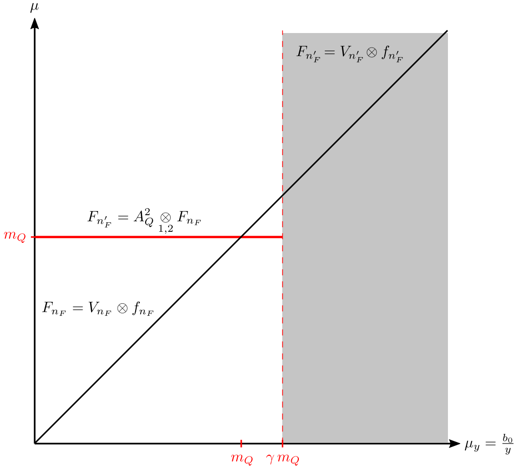

- Above $\mu_y = \gamma\, m_Q$ the DPD is initialized for $n_F + 1$ massless flavours with a $n_F + 1$ flavour PDF.

DPDs in the massless scheme.

Consider $n_F = 5$ LO splitting DPDs at $\mu_1 = \mu_2 = m_{\text{dijet}} = 25\,\text{GeV}$ initialized with the scheme shown in the previous slide:

$$F_{b\bar{b}}(x_1 = x_2 = m_{\text{dijet}}/\sqrt{s},\, y,\, m_{\text{dijet}})$$

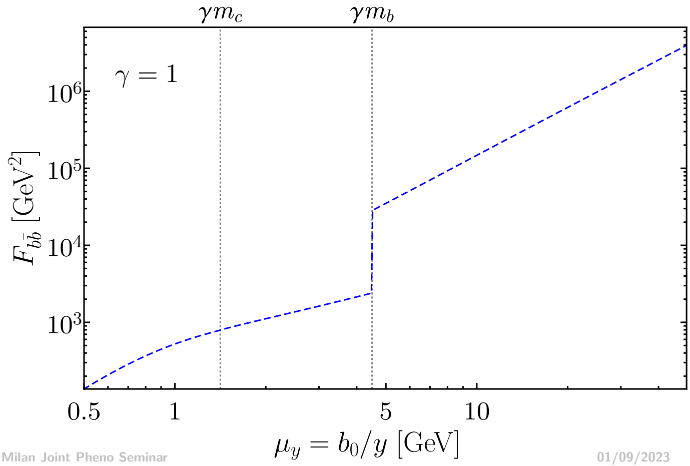

- Below $\mu_y = m_b$ the $b\bar{b}$ DPD is produced only by flavour matching and evolution.
- Above $\mu_y = m_b$ the $b\bar{b}$ DPD is produced by a direct (massless) $g \to q\bar{q}$ splitting.

DPDs in the massless scheme.

Consider $n_F = 5$ LO splitting DPDs at $\mu_1 = \mu_2 = m_{\text{dijet}} = 25\,\text{GeV}$ initialized with the scheme shown in the previous slide:

$$F_{gb}(x_1 = x_2 = m_{\text{dijet}}/\sqrt{s},\, y,\, m_{\text{dijet}})$$

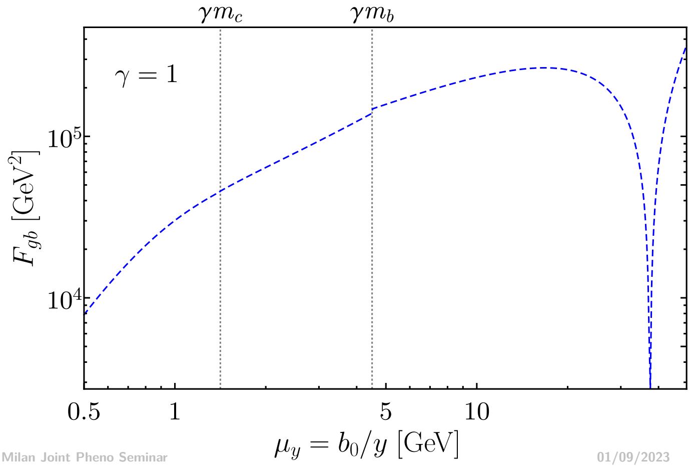

- At LO the gb DPD is produced by a direct splitting only for $\mu_y > \gamma m_b$.
- Heavy quark effects in the splitting seem to be unimportant.

A more realistic treatment of quark mass effects.

In the splitting DPDs one can distinguish three regions of μ_{split}:

$\mu_{\text{split}} \ll m_Q$:

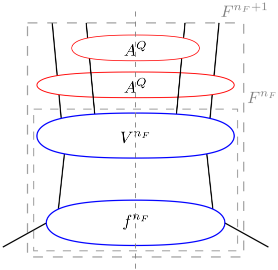

- In the splitting the heavy quarks decouple.
- $n_F + 1$ DPDs obtained by flavour matching.

$\mu_{\text{split}} \sim m_Q$:

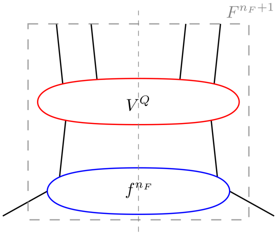

- Heavy quarks treated as massive in the splitting kernel V^Q.

$\mu_{\text{split}} \gg m_Q$:

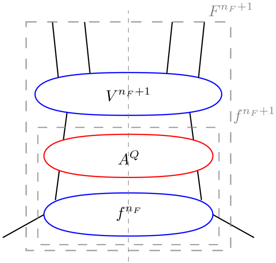

- Heavy quarks can be treated as massless in the splitting.

Massive DPD splitting kernels.

Just like the massless V^{n_F} kernels the massive V^{Q} kernels can be computed in perturbation theory!

At leading order the only splitting with massive quarks is $g \to Q\bar{Q}$, where the kernel reads:

$$V^{(1)}_{Q\bar{Q},g}(z_1, z_2, m_Q, y) = T_f\, (m_Q\, y)^2 \left[(z_1^2 + z_2^2)\, K_1^2(m_Q\, y) + K_0^2(m_Q\, y) \right] \delta(1 - z_1 - z_2)$$

with the following limiting behaviour for small and large μ_{split} (corresponding to large and small $m_Q\, y$, respectively):

$$\mu_{\text{split}} \ll m_Q : \qquad V^{(1)}_{Q\bar{Q},g}(z, m_Q, y) \longrightarrow 0$$

$$\mu_{\text{split}} \gg m_Q : \qquad V^{(1)}_{Q\bar{Q},g}(z_1, z_2, m_Q, y) \longrightarrow T_f (z_1^2 + z_2^2)\, \delta(1 - z_1 - z_2) = V^{(1)}_{q\bar{q},g}(z_1, z_2)$$

$\longrightarrow$ The massive kernel interpolates between the regions where the heavy quark decouples and where it can be treated as massless!

One heavy flavour.

Consider now the initialization of a splitting DPD with one heavy flavour (where $\alpha \ll 1$ and $\beta \gg 1$):

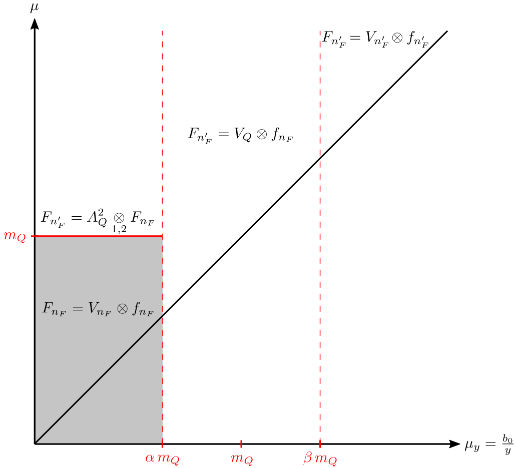

- Below $\mu_y = \alpha\, m_Q$ the DPD is initialized for n_F massless flavours with a n_F flavour PDF.

One heavy flavour.

Consider now the initialization of a splitting DPD with one heavy flavour (where $\alpha \ll 1$ and $\beta \gg 1$):

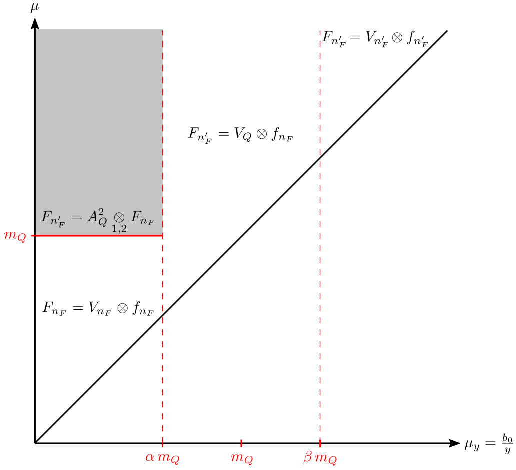

- Below $\mu_y = \alpha\, m_Q$ the $n_F + 1$ DPD is obtained by flavour matching.

One heavy flavour.

Consider now the initialization of a splitting DPD with one heavy flavour (where $\alpha \ll 1$ and $\beta \gg 1$):

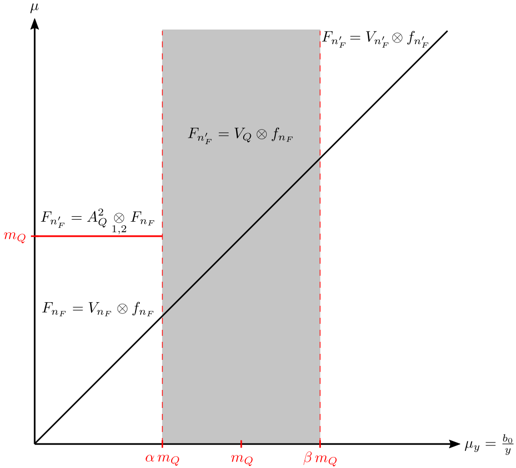

- For $\alpha\, m_Q < \mu_y < \beta\, m_Q$ the DPD is initialized for n_F massless and one massive flavours with a n_F flavour PDF.

One heavy flavour.

Consider now the initialization of a splitting DPD with one heavy flavour (where $\alpha \ll 1$ and $\beta \gg 1$):

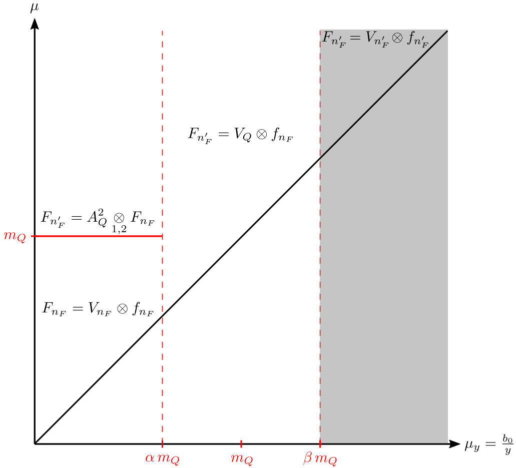

- Above $\mu_y = \beta\, m_Q$ the DPD is initialized for $n_F + 1$ massless flavours with a $n_F + 1$ flavour PDF.

One heavy flavour.

Consider now the initialization of a splitting DPD with one heavy flavour (where $\alpha \ll 1$ and $\beta \gg 1$):

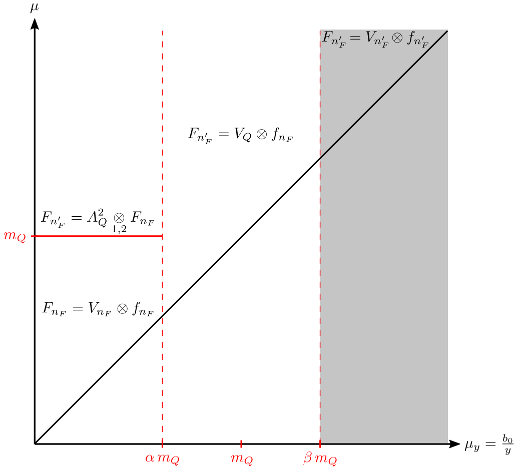

- Above $\mu_y = \beta\, m_Q$ the DPD is initialized for $n_F + 1$ massless flavours with a $n_F + 1$ flavour PDF.

What happens for charm and bottom which have to be treated as massive simultaneously?

Two heavy flavours: charm and bottom.

Consider now the initialization of a splitting DPD with massive c and b quarks:

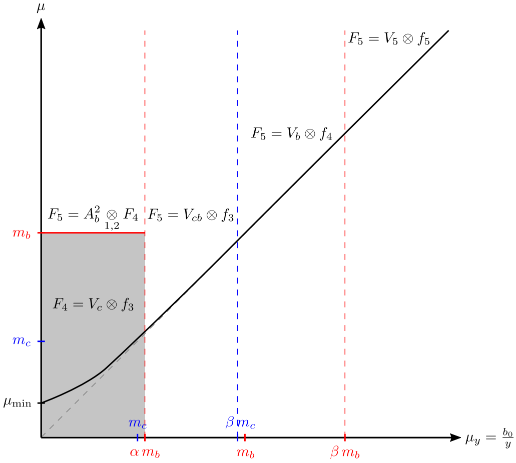

- Below $\mu_y = \alpha\, m_b$ the DPD is initialized for 3 massless and one heavy flavours with a 3 flavour PDF.

Two heavy flavours: charm and bottom.

Consider now the initialization of a splitting DPD with massive c and b quarks:

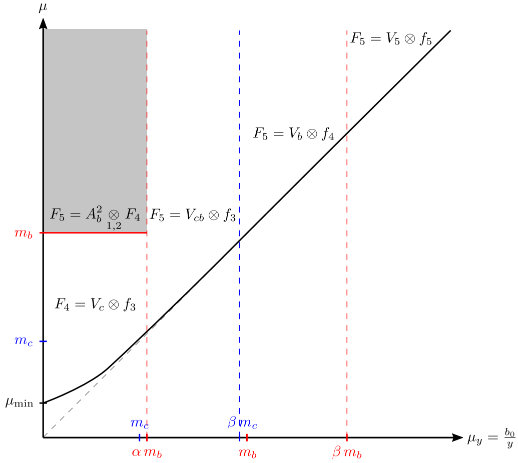

- Below $\mu_y = \alpha\, m_b$ the 5 flavour DPD is obtained by flavour matching.

Two heavy flavours: charm and bottom.

Consider now the initialization of a splitting DPD with massive c and b quarks:

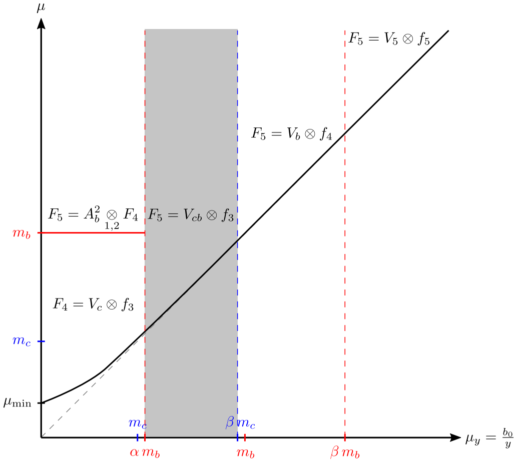

- For $\alpha\, m_b < \mu_y < \beta\, m_c$ the DPD is initialized for 3 massless and two massive flavours with a 3 flavour PDF.

Two heavy flavours: charm and bottom.

Consider now the initialization of a splitting DPD with massive c and b quarks:

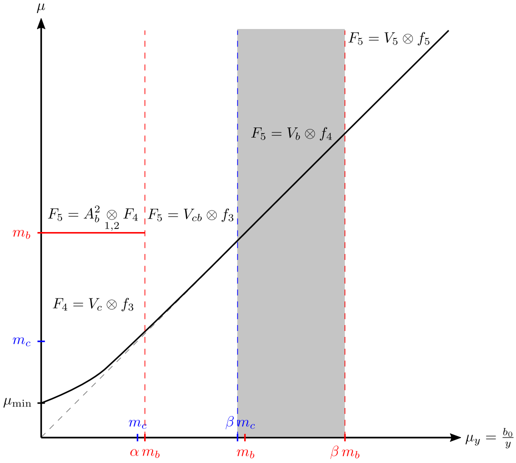

- For $\beta\, m_c < \mu_y < \beta\, m_b$ the DPD is initialized for 4 massless and one massive flavours with a 4 flavour PDF.

Two heavy flavours: charm and bottom.

Consider now the initialization of a splitting DPD with massive c and b quarks:

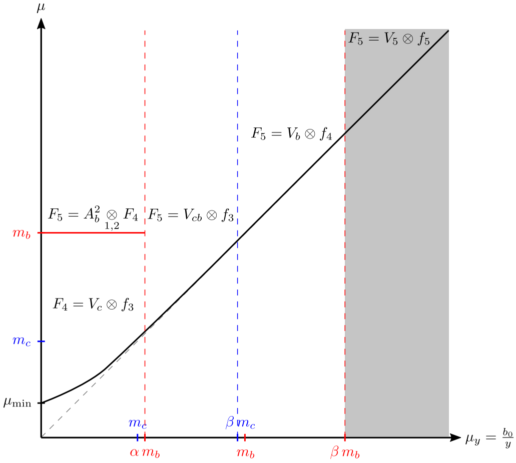

- Above $\mu_y = \beta\, m_b$ the DPD is initialized for 5 massless flavours with a 5 flavour PDF.

Two heavy flavours: charm and bottom.

Consider now the initialization of a splitting DPD with massive c and b quarks:

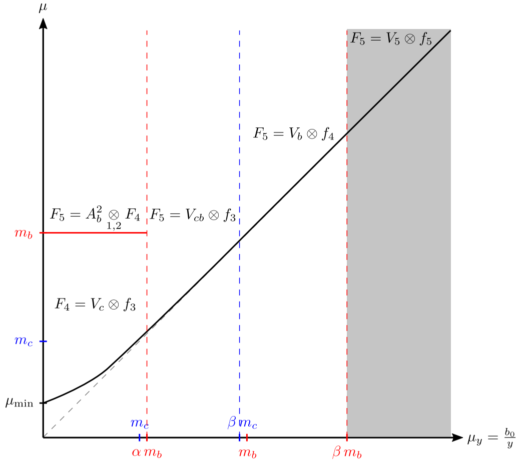

- Above $\mu_y = \beta\, m_b$ the DPD is initialized for 5 massless flavours with a 5 flavour PDF.

Let's see how the DPDs look like in this scheme!

DPDs in the massive scheme.

Consider now $n_F = 5$ LO splitting DPDs at $\mu_1 = \mu_2 = m_{\text{dijet}} = 25\,\text{GeV}$ for dijet production, initialized with the scheme shown in the previous slide (for different α and β):

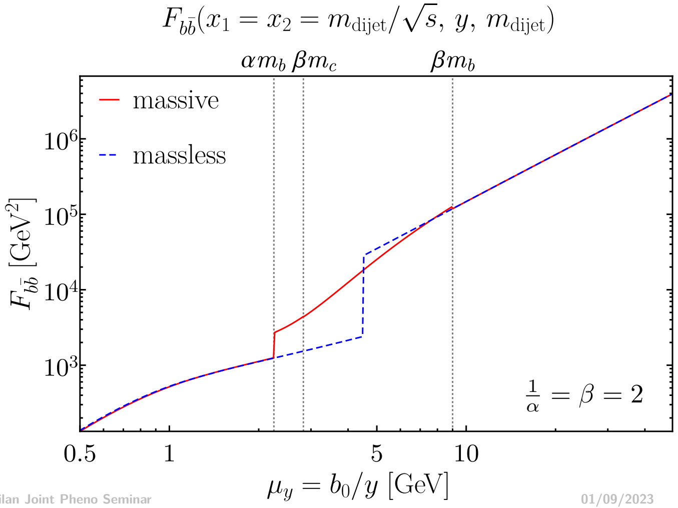

- DPDs still discontinuous, but greatly improved compared to the massless scheme!

DPDs in the massive scheme.

Consider now $n_F = 5$ LO splitting DPDs at $\mu_1 = \mu_2 = m_{\text{dijet}} = 25\,\text{GeV}$ for dijet production, initialized with the scheme shown in the previous slide (for different α and β):

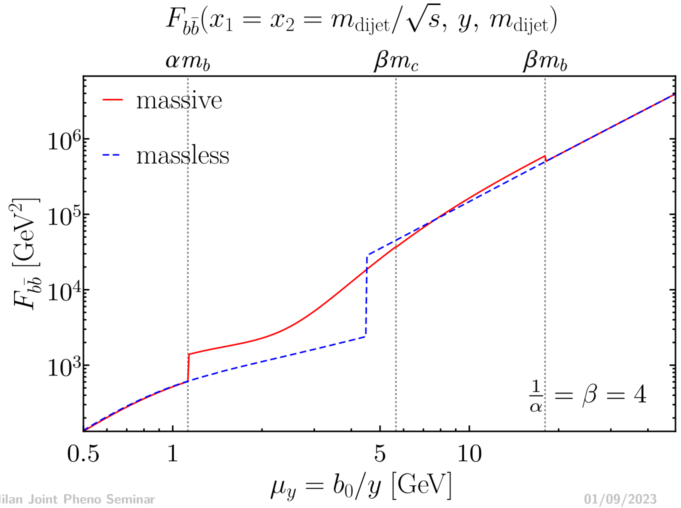

- DPDs still discontinuous, but greatly improved compared to the massless scheme!

DPDs in the massive scheme.

Consider now $n_F = 5$ LO splitting DPDs at $\mu_1 = \mu_2 = m_{\text{dijet}} = 25\,\text{GeV}$ for dijet production, initialized with the scheme shown in the previous slide (for different α and β):

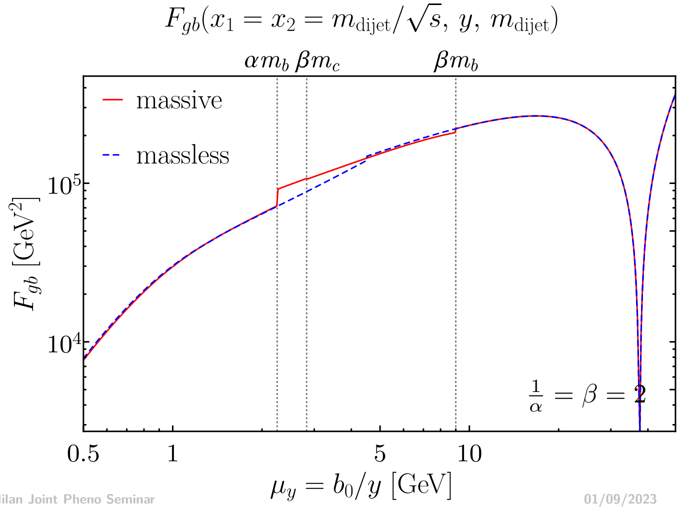

- Increased discontinuity for gb at $\mu_y = \alpha m_b$ due to direct production of $\bar{b}b$ DPD!
- Increased discontinuity for gb at $\mu_y = \beta m_b$ due to more production modes in the massless case!

DPDs in the massive scheme.

Consider now $n_F = 5$ LO splitting DPDs at $\mu_1 = \mu_2 = m_{\text{dijet}} = 25\,\text{GeV}$ for dijet production, initialized with the scheme shown in the previous slide (for different α and β):

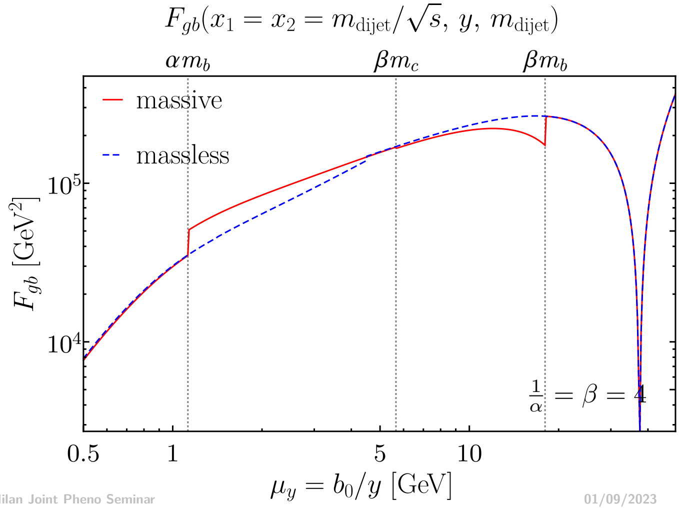

- Increased discontinuity for gb at $\mu_y = \alpha m_b$ due to direct production of $\bar{b}b$ DPD!
- Increased discontinuity for gb at $\mu_y = \beta m_b$ due to more production modes in the massless case!

DPDs in the massive scheme.

Consider now $n_F = 5$ LO splitting DPDs at $\mu_1 = \mu_2 = m_{\text{dijet}} = 25\,\text{GeV}$ for dijet production, initialized with the scheme shown in the previous slide (for different α and β):

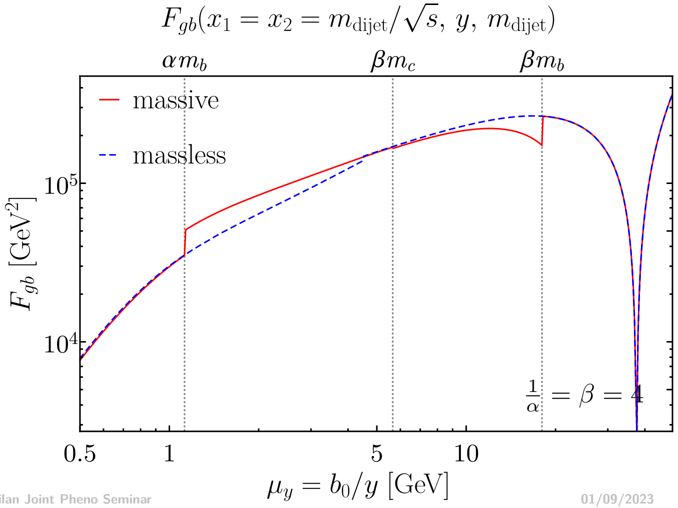

- Smallest discontinuities for $\beta = 2$ and $\alpha = \frac{1}{4}$!
- Seen also in other DPDs and at different scales, cf. backup slides.

DPD luminosities.

In order to study the effect of heavy quarks on DPS cross sections, consider DPD luminosities, i.e. products of DPDs integrated over y:

$$\mathcal{L}_{a_1 a_2 b_1 b_2}(x_{1a}, x_{2a}, x_{1b}, x_{2b}; \nu, \mu_1, \mu_2) = \int_{b_0/\nu} \mathrm{d}^2\boldsymbol{y}\, F_{a_1 a_2}(x_{1a}, x_{2a}, y; \mu_1, \mu_2) F_{b_1 b_2}(x_{1b}, x_{2b}, y; \mu_1, \mu_2)$$

where the lower cut-off regulates the y^{-4} splitting singularity.

Here we include also “intrinsic” non-splitting contributions to the DPDs, modelled as:

$$F^{\text{int}}_{a_1 a_2}(x_1, x_2, y; \mu_1, \mu_2) = \frac{(1 - x_1 - x_2)^2}{(1 - x_1)^2 (1 - x_2)^2} \frac{\exp\left(-\frac{y^2}{4h_{a_1 a_2}}\right)}{4\pi h_{a_1 a_2}} f_{a_1}(x_1, \mu_1)\, f_{a_2}(x_2, \mu_2)$$

In the following all possible combinations containing splitting DPDs are considered:

DPD luminosities.

In order to study the effect of heavy quarks on DPS cross sections, consider DPD luminosities, i.e. products of DPDs integrated over y:

$$\mathcal{L}_{a_1 a_2 b_1 b_2}(x_{1a}, x_{2a}, x_{1b}, x_{2b}; \nu, \mu_1, \mu_2) = \int_{b_0/\nu} \mathrm{d}^2\boldsymbol{y}\, F_{a_1 a_2}(x_{1a}, x_{2a}, y; \mu_1, \mu_2) F_{b_1 b_2}(x_{1b}, x_{2b}, y; \mu_1, \mu_2)$$

where the lower cut-off regulates the y^{-4} splitting singularity.

Here we include also "intrinsic" non-splitting contributions to the DPDs, modelled as:

$$F^{\text{int}}_{a_1 a_2}(x_1, x_2, y; \mu_1, \mu_2) = \frac{(1 - x_1 - x_2)^2}{(1 - x_1)^2 (1 - x_2)^2} \frac{\exp\left(-\frac{y^2}{4h_{a_1 a_2}}\right)}{4\pi h_{a_1 a_2}} f_{a_1}(x_1, \mu_1)\, f_{a_2}(x_2, \mu_2)$$

split x split (1v1), split x int (1v2), int x split (2v1).

DPD luminosities in the massive scheme.

Consider now ratios of LO DPD luminosities for dijet production with different scheme parameters:

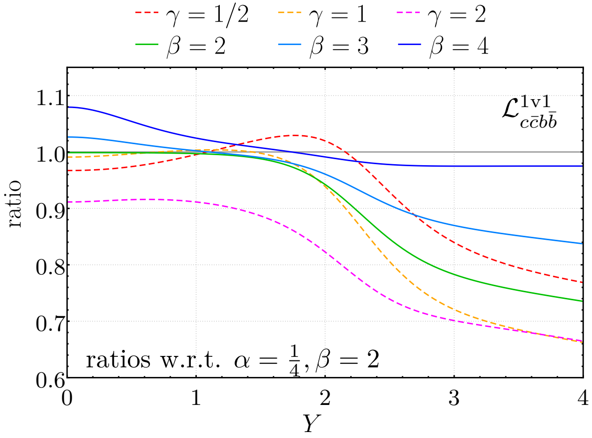

Jets at rapidities Y and $-Y$:

$$x_{1a} = \frac{m_{\text{dijet}}}{\sqrt{s}} \exp(Y)$$

$$x_{2a} = \frac{m_{\text{dijet}}}{\sqrt{s}} \exp(-Y)$$

$$x_{1b} = \frac{m_{\text{dijet}}}{\sqrt{s}} \exp(-Y)$$

$$x_{2b} = \frac{m_{\text{dijet}}}{\sqrt{s}} \exp(Y)$$

DPD luminosities in the massive scheme.

Consider now ratios of LO DPD luminosities for dijet production with different scheme parameters:

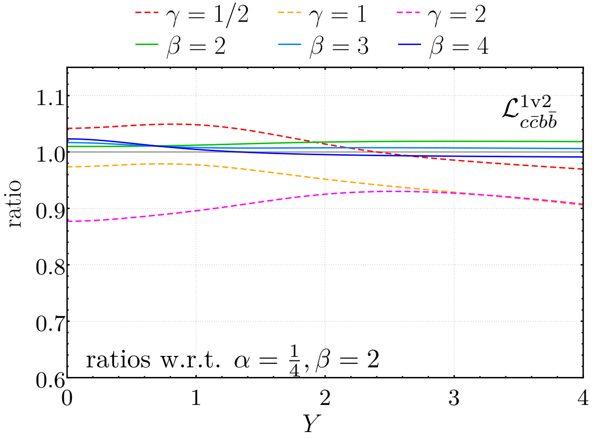

Jets at rapidities Y and $-Y$:

$$x_{1a} = \frac{m_{\text{dijet}}}{\sqrt{s}} \exp(Y)$$

$$x_{2a} = \frac{m_{\text{dijet}}}{\sqrt{s}} \exp(-Y)$$

$$x_{1b} = \frac{m_{\text{dijet}}}{\sqrt{s}} \exp(-Y)$$

$$x_{2b} = \frac{m_{\text{dijet}}}{\sqrt{s}} \exp(Y)$$

DPD luminosities in the massive scheme.

Consider now ratios of LO DPD luminosities for dijet production with different scheme parameters:

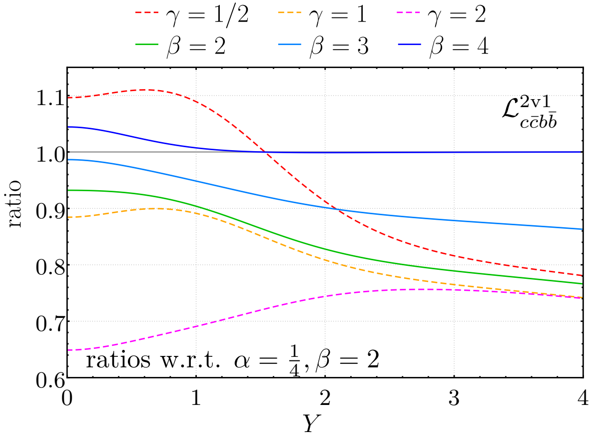

Jets at rapidities Y and $-Y$:

$$x_{1a} = \frac{m_{\text{dijet}}}{\sqrt{s}} \exp(Y)$$

$$x_{2a} = \frac{m_{\text{dijet}}}{\sqrt{s}} \exp(-Y)$$

$$x_{1b} = \frac{m_{\text{dijet}}}{\sqrt{s}} \exp(-Y)$$

$$x_{2b} = \frac{m_{\text{dijet}}}{\sqrt{s}} \exp(Y)$$

DPD luminosities in the massive scheme.

Consider now ratios of LO DPD luminosities for dijet production with different scheme parameters:

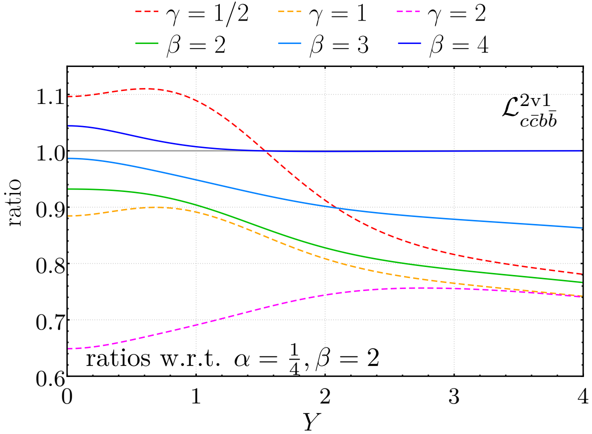

Jets at rapidities Y and $-Y$:

$$x_{1a} = \frac{m_{\text{dijet}}}{\sqrt{s}} \exp(Y)$$

$$x_{2a} = \frac{m_{\text{dijet}}}{\sqrt{s}} \exp(-Y)$$

$$x_{1b} = \frac{m_{\text{dijet}}}{\sqrt{s}} \exp(-Y)$$

$$x_{2b} = \frac{m_{\text{dijet}}}{\sqrt{s}} \exp(Y)$$

$\longrightarrow$ Smaller dependence of luminosities on α and β compared to γ!

DPD luminosities in the massive scheme: Scale dependence.

Finally consider the dependence of DPD luminosities involving LO splitting DPDs on the scale μ_{split} (varied by a factor of 2):

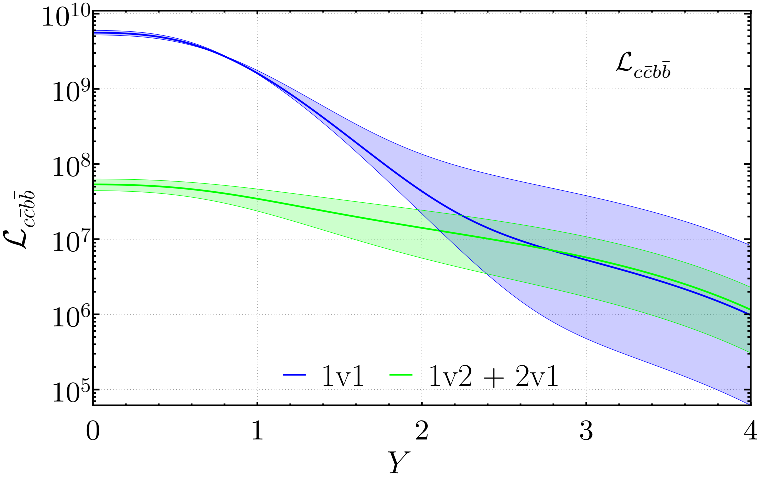

- Note that the 1v1 luminosities contain the squared uncertainties of the splitting DPDs!

DPD luminosities in the massive scheme: Scale dependence.

Finally consider the dependence of DPD luminosities involving LO splitting DPDs on the scale μ_{split} (varied by a factor of 2):

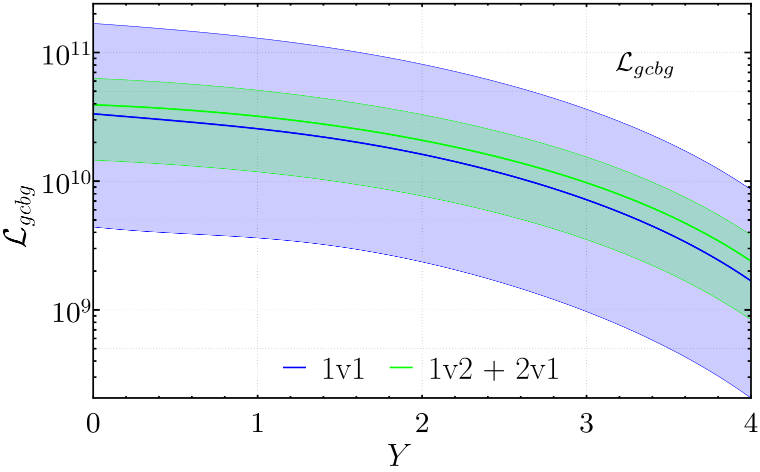

- Note that the 1v1 luminosities contain the squared uncertainties of the splitting DPDs!

DPD luminosities in the massive scheme: Scale dependence.

Finally consider the dependence of DPD luminosities involving LO splitting DPDs on the scale μ_{split} (varied by a factor of 2):

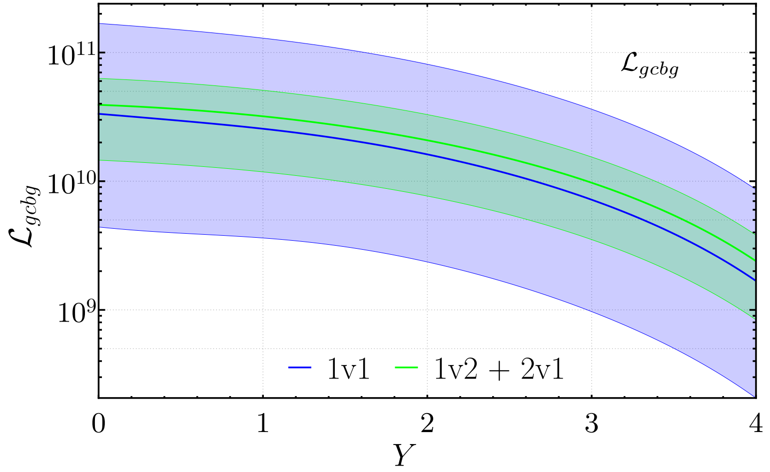

- Large scale uncertainties hint at importance of higher order splitting!

DPD luminosities in the massive scheme: Scale dependence.

Finally consider the dependence of DPD luminosities involving LO splitting DPDs on the scale μ_{split} (varied by a factor of 2):

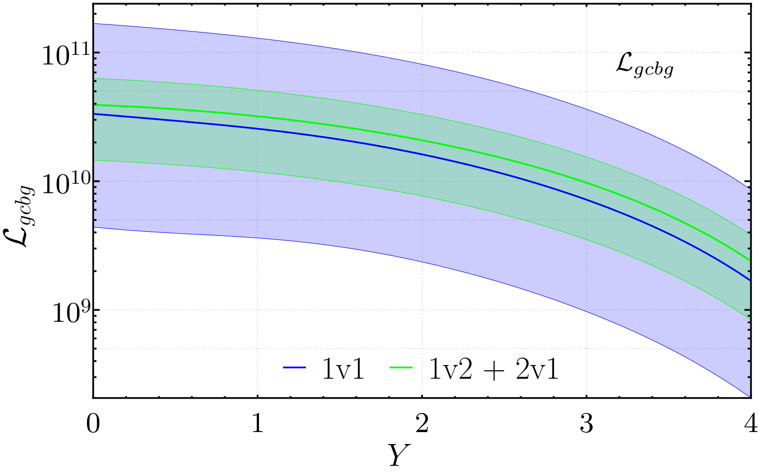

- Massless NLO kernels already calculated! [Diehl, Gaunt, PP, Schäfer, 2019; Diehl, Gaunt, PP, 2021]

DPD luminosities in the massive scheme: Scale dependence.

Finally consider the dependence of DPD luminosities involving LO splitting DPDs on the scale μ_{split} (varied by a factor of 2):

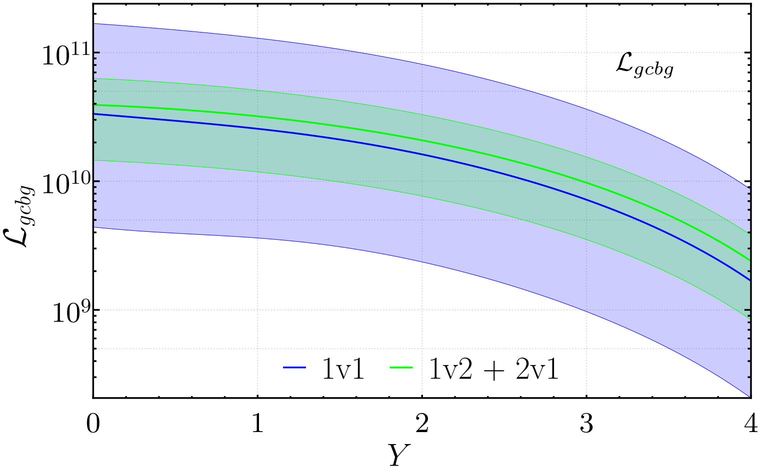

- Massive NLO kernels still unknown!

Constraints for the massive NLO kernels.

For now a full calculation of the massive NLO kernels is out of reach for us (involves massive two-loop diagrams).

$\longrightarrow$ construct approximate solutions!

To this end make use of the following constraints:

- RGE dependence of the massive kernels.
- Small and large distance limits of the massive kernels.
- DPD number and momentum sum rules.

The limiting behaviour and RGE dependence are uniquely fixed by these constraints, while the DPD sum rules constrain also intermediate inter parton distances!

RGE dependence of the massive NLO kernels.

The RGE dependence of the massive NLO kernels is completely fixed by LO perturbative ingredients:

Scale dependence of the massive NLO kernels:

$$\frac{\mathrm{d}}{\mathrm{d}\log\mu^2} V^{Q,n_F(2)}_{a_1a_2,a_0} = \sum_{b_1} P^{n_F+1(0)}_{a_1b_1} \underset{1}{\otimes} V^{Q(1)}_{b_1a_2,a_0} + \sum_{b_2} P^{n_F+1(0)}_{a_2b_2} \underset{2}{\otimes} V^{Q(1)}_{a_1b_2,a_0}$$
$$- \sum_{b_0} V^{Q(1)}_{a_1a_2,b_0} \underset{12}{\otimes} P^{n_F(0)}_{b_0a_0} + \frac{\beta_0^{n_F+1}}{2} V^{Q(1)}_{a_1a_2,a_0}$$
$$= v^{n_F,\,\mathrm{RGE}}_{a_1a_2,a_0}$$

where the $V^{Q(1)}$ are the massive LO kernels and the $P^{n_F(0)}_{ab}$ are the LO DGLAP kernels.

Limiting behaviour of the massive NLO kernels.

For small and large interparton distances the massive kernels can be expressed in terms of convolutions of massless kernels and flavour matching kernels:

Small distance limit:

$$V^{Q,n_F(2)}_{a_1 a_2, a_0} \xrightarrow{y \to 0} \delta^{n_F}_{a_0 l} \, V^{n_F+1(2)}_{a_1 a_2, a_0} + \sum_{b_0} V^{n_F+1(1)}_{a_1 a_2, b_0} \underset{12}{\otimes} A^{Q(1)}_{b_0 a_0} \,,$$

Large distance limit:

$$V^{Q,n_F(2)}_{a_1 a_2, a_0} \xrightarrow{y \to \infty} V^{n_F(2)}_{a_1 a_2, a_0} + \sum_{b_1} A^{Q(1)}_{a_1 b_1} \underset{1}{\otimes} V^{(1)}_{b_1 a_2, a_0} + \sum_{b_2} A^{Q(1)}_{a_2 b_2} \underset{2}{\otimes} V^{(1)}_{a_1 b_2, a_0} + A^{Q(1)}_{\alpha} \, V^{(1)}_{a_1 a_2, a_0} \,.$$

Sum rules for the massive NLO kernels.

The Gaunt-Stirling DPD sum rules can be used to derive sum rules for the massive kernels:

Momentum sum rule:

$$
\begin{aligned}
&\sum_{a_2} \int_2 X_2 \int_{y_\beta}^{y_\alpha} \mathrm{d}^2 y \, V^{Q,n_F(2)}_{a_1 a_2, a_0} = (1 - X) \, A^{Q(2)}_{a_1 a_0} \\
&\quad + \sum_{a_2} \int_2 X_2 \left[U^{n_F(2)}_{a_1 a_2, a_0}(r_\alpha) - U^{n_F+1(2)}_{a_1 a_2, a_0}(r_\beta) \right] + A^{(1)}_{\alpha} \sum_{a_2} \int_2 X_2 \, U^{(1)}_{a_1 a_2, a_0}(r_\alpha) \\
&\quad + \sum_{b_1, a_2} A^{Q(1)}_{a_1 b_1} \underset{1}{\otimes} \left(\int_2 X_2 \, U^{(1)}_{b_1 a_2, a_0}(r_\alpha) \right) - \sum_{a_2, b_0} \left(\int_2 X_2 \, U^{(1)}_{a_1 a_2, b_0}(r_\beta) \right) \otimes \left(X A^{Q(1)}_{b_0 a_0} \right)
\end{aligned}
$$

Sum rules for the massive NLO kernels.

The Gaunt-Stirling DPD sum rules can be used to derive sum rules for the massive kernels:

Number sum rule:

$$\int\limits_2 \int_{y_\beta}^{y_\alpha} \mathrm{d}^2 y \frac{1}{\pi y^2} V^{Q,n_F(2)}_{a_1 a_{2v}, a_0} = \left(\delta_{a_1 \bar{a}_2} - \delta_{a_1 a_2} - \delta_{a_2 \bar{a}_0} + \delta_{a_2 a_0}\right) A^{Q(2)}_{a_1 a_0}$$
$$+ \int\limits_2 \left[U^{n_F(2)}_{a_1 a_{2v}, a_0}(r_\alpha) - U^{n_F+1(2)}_{a_1 a_{2v}, a_0}(r_\beta)\right] + A^{(1)}_\alpha \int\limits_2 U^{(1)}_{a_1 a_{2v}, a_0}(r_\alpha)$$
$$+ \sum_{b_1} A^{Q(1)}_{a_1 b_1} \otimes \left(\int\limits_2 U^{(1)}_{b_1 a_{2v}, a_0}(r_\alpha)\right) - \sum_{b_2} \left(\int\limits_2 U^{(1)}_{a_1 a_{2v}, b_0}(r_\beta)\right) \otimes A^{Q(1)}_{b_0 a_0}$$

Quark mass effects in the $1 \to 2$ splitting.

Ansatz for the massive NLO kernels.

The following ansatz fulfils the RGE and limiting behaviour constraints:

$$V^{Q,n_F(2)}_{a_1a_2,a_0} = V^{n_F[2,0]}_{a_1a_2,a_0} + V^{n_F[2,1]}_{a_1a_2,a_0} \log\frac{m_Q^2}{\mu_y^2} + k_{00}(y\, m_Q)\, v^{n_F,I}_{a_1a_2,a_0}(z_1,z_2)$$
$$+ k_{11}(y m_Q)\left(V^{n_F+1[2,0]}_{a_1a_2,a_0} - V^{n_F[2,0]}_{a_1a_2,a_0}\right) - k_{02}(y m_Q)\left(V^{n_F+1[2,1]}_{a_1a_2,a_0} - V^{n_F[2,1]}_{a_1a_2,a_0}\right)$$
$$+ \log\frac{\mu^2}{m_Q^2}\, v^{n_F,\mathrm{RGE}}_{a_1a_2,a_0}(z_1,z_2)\,,$$

where

$$k_{ij}(w) = w^2 K_i(w) K_j(w)\,.$$

$\longrightarrow$ Sum rules can be used to constrain $v^{n_F,I}_{a_1a_2,a_0}$!

Part V

Summary.

Summary.

Why DPS is interesting:

- Contributes background to the search for new physics.
- Relative importance of DPS increases with collision energy (relevant for possible FCC).
- DPS gives access to information about correlation between partons inside hadrons.

A framework for DPS:

- Factorization proof for double Drell-Yan.
  [Diehl, Ostermeier, and Schäfer, 2011; Diehl, Gaunt, Ostermeier, Plößl, and Schäfer, 2015; Diehl and Nagar, 2019]
- Subtraction formalism for a consistent combination of DPS and SPS cross sections.
  [Diehl, Gaunt, and Schönwald, 2017]

Properties of DPDs:

- Definition in terms of proton matrix elements of a product of twist-2 operators.
- Rapidity dependence governed by CS-equation (consequence of rapidity subtraction).
- Renormalisation scale dependence governed by double DGLAP equation.

Summary.

For small interparton distances DPDs can be matched onto PDFs with perturbative $1 \to 2$ splitting kernels, yielding a valuable constraint for the largely unknown DPDs!

NLO calculation of the $1 \to 2$ splitting kernels: [Diehl, Gaunt, Plößl, and Schäfer, 2019; Diehl, Gaunt, and Plößl, 2021]

- Calculated the unpolarised NLO small y splitting kernels ${}^{R_1 R_2}V^{(2)}_{a_1 a_2, a_0}$ for all parton and colour channels.
- Used different rapidity regulator schemes, providing a strong cross check.
- First application of the Collins regulator in a two loop calculation.

NLO $1 \to 2$ splitting kernels make it possible to construct NLO DPD models and extend the SPS-DPS subtraction formalism to NLO!

Treatment of massive quarks in the small distance splitting: [Diehl, Nagar, and Plößl, 2022]

- Heavy quark decouples for $\mu_{\text{split}} \ll m_Q$.
- Heavy quark treated as massive for $\mu_{\text{split}} \sim m_Q$.
- Heavy quark treated as massless for $\mu_{\text{split}} \gg m_Q$.

Including quark mass effects leads to DPDs with smaller discontinuities and stabilizes DPD luminosities compared to the purely massless case!

Summary.

For small interparton distances DPDs can be matched onto PDFs with perturbative $1 \to 2$ splitting kernels, yielding a valuable constraint for the largely unknown DPDs!

NLO calculation of the $1 \to 2$ splitting kernels: [Diehl, Gaunt, Plößl, and Schäfer, 2019; Diehl, Gaunt, and Plößl, 2021]

- Calculated the unpolarised NLO small y splitting kernels ${}^{R_1 R_2}V^{(2)}_{a_1 a_2, a_0}$ for all parton and colour channels.
- Used different rapidity regulator schemes, providing a strong cross check.
- First application of the Collins regulator in a two loop calculation.

NLO $1 \to 2$ splitting kernels make it possible to construct NLO DPD models and extend the SPS-DPS subtraction formalism to NLO!

Treatment of massive quarks in the small distance splitting: [Diehl, Nagar, and Plößl, 2022]

- Heavy quark decoupled for $\mu_{\text{split}} \ll m_Q$.
- Heavy quark treated as massive for $\mu_{\text{split}} \sim m_Q$.
- Heavy quark treated as massless for $\mu_{\text{split}} \gg m_Q$.

Including quark mass effects leads to DPDs with smaller discontinuities and stabilizes DPD luminosities compared to the purely massless case!

Thank you for your attention!

Part VI

Backup.

Rescaling of the rapidity parameter.

The rapidity parameters ζ_p and $\zeta_{\bar{p}}$ in this work are normalised as:

$$\zeta_p \zeta_{\bar{p}} = (2p^+ \bar{p}^-)^2 = s^2 \,,$$

which differs from the convention in the TMD case

$$\zeta \bar{\zeta} = x^2 \bar{x}^2 (2p^+ \bar{p}^-)^2 = Q^4 \,,$$

where the rapidity parameters are normalized w.r.t. the extracted parton, which would be awkward in the DPD case where parton momenta often appear in convolution integrals.

$\longrightarrow$ need to rescale the rapidity parameter in renormalisation factors and evolution kernels!

$\longrightarrow$ reason: can only depend on the plus-momentum $x_i p^+$ of the parton to which they refer!

Quark mass effects in the $1 \to 2$ splitting.

F_{gb}: massless vs. massive scheme

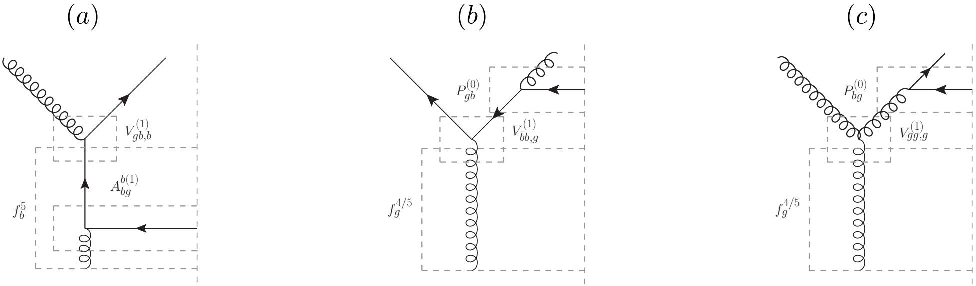

(a)
- Only contributes in the massless scheme.
- DPD produced by direct splitting, no evolution necessary.

(b)
- Contributes in the massive and massless schemes.
- DPD only produced by evolution.

(c)
- Contributes in the massive and massless schemes.
- DPD only produced by evolution.

- Contributions (b) and (c) vanish when the splitting scale is identical to the target scale!

F_{gb}: massless vs. massive scheme

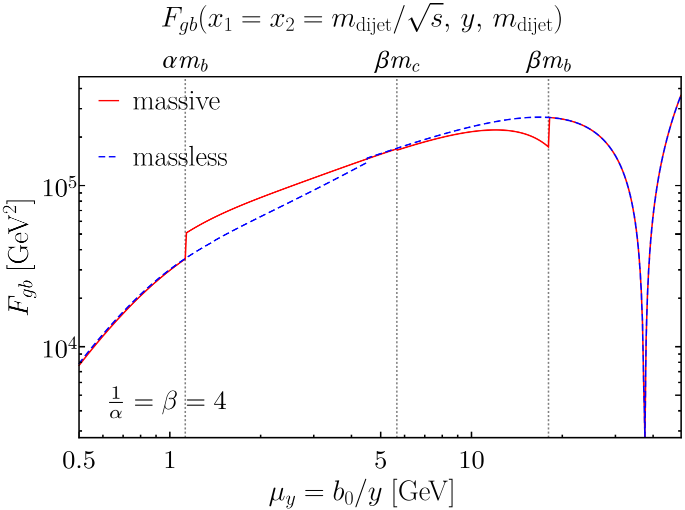

Scale dependence of splitting DPDs: in depth.

In order to understand the μ_{split} dependence of LO DPD luminosities involving $q\bar{q}$ DPDs consider the scale variation of the involved DPDs ($x_1 = \frac{m_W}{\sqrt{s}} \exp Y$, $x_2 = \frac{m_W}{\sqrt{s}} \exp -Y$):

Central rapidity ($Y = 0$):

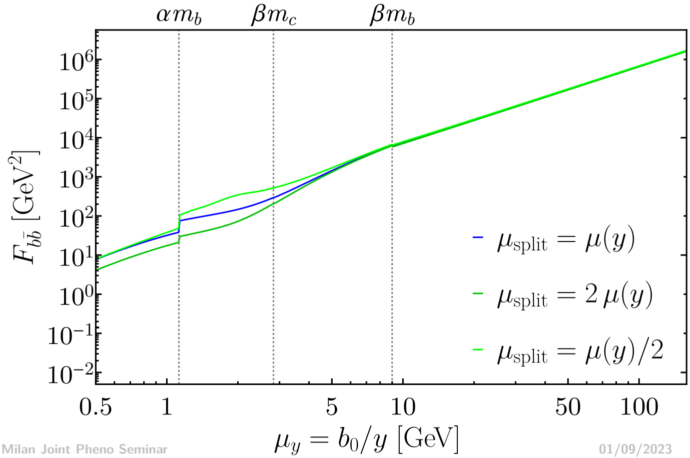

Scale dependence of splitting DPDs: in depth.

In order to understand the μ_{split} dependence of LO DPD luminosities involving $q\bar{q}$ DPDs consider the scale variation of the involved DPDs ($x_1 = \frac{m_W}{\sqrt{s}} \exp Y$, $x_2 = \frac{m_W}{\sqrt{s}} \exp -Y$):

Central rapidity ($Y = 0$), only $g \to q\bar{q}$ splitting:

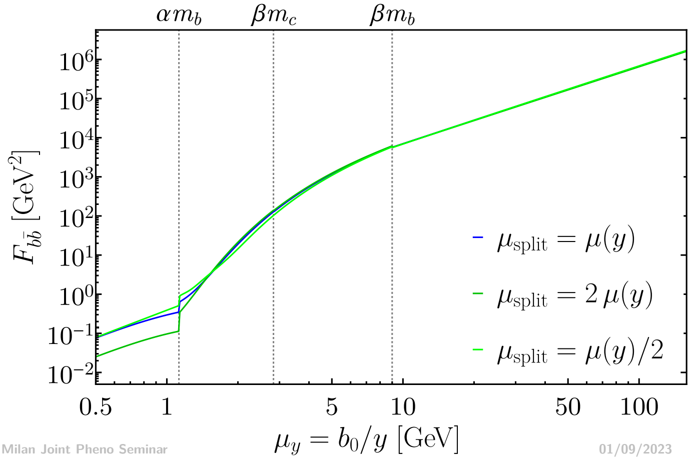

- Contribution from $g \to gg$ and $q \to qg, gq$ splitting and evolution negligible for central rapidity ($x_1 = x_2$).
- Only scale variation from initial gluon PDF.

Scale dependence of splitting DPDs: in depth.

In order to understand the μ_{split} dependence of LO DPD luminosities involving $q\bar{q}$ DPDs consider the scale variation of the involved DPDs ($x_1 = \frac{m_W}{\sqrt{s}} \exp Y$, $x_2 = \frac{m_W}{\sqrt{s}} \exp -Y$):

Non-central rapidity ($Y = 3$):

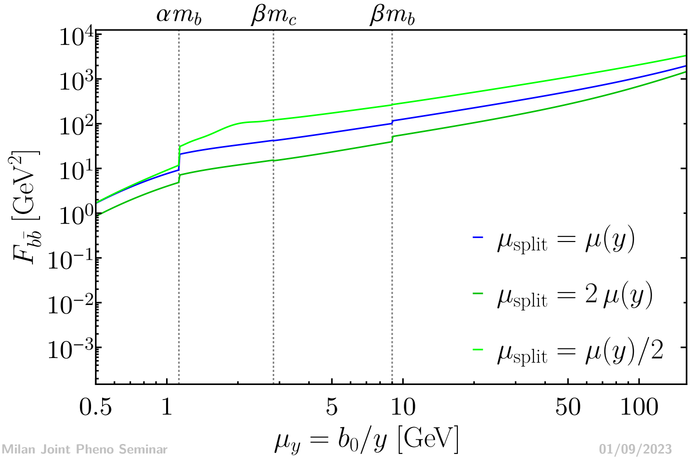

Scale dependence of splitting DPDs: in depth.

In order to understand the μ_{split} dependence of LO DPD luminosities involving $q\bar{q}$ DPDs consider the scale variation of the involved DPDs ($x_1 = \frac{m_W}{\sqrt{s}} \exp Y$, $x_2 = \frac{m_W}{\sqrt{s}} \exp -Y$):

Non-central rapidity ($Y = 3$), only $g \to q\bar{q}$ splitting:

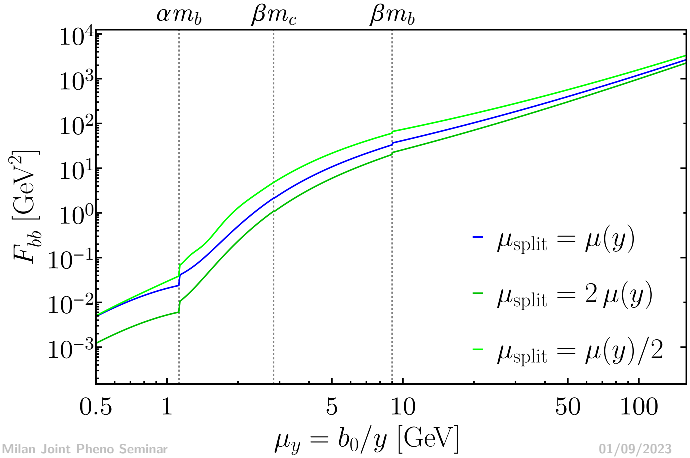

- Sizeable contribution from $g \to gg$ and $q \to qg, gq$ splitting and evolution for non-central rapidity ($x_1 \ll x_2$).
- In addition to scale variation from initial gluon PDF also uncertainties from evolution.

DPD luminosities in the massive scheme: Matching scale dependence.

Finally consider the dependence of LO DPD luminosities for dijet production on the flavour matching scales (at LO, varied by a factor of 2):

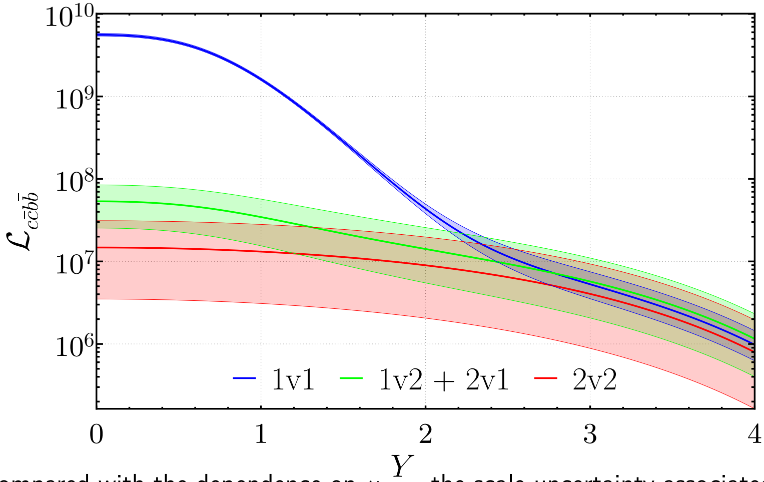

$$x_{1a} = \frac{m_W}{\sqrt{s}} \exp(Y)$$

$$x_{2a} = \frac{m_W}{\sqrt{s}} \exp(-Y)$$

$$x_{1b} = \frac{m_W}{\sqrt{s}} \exp(-Y)$$

$$x_{2b} = \frac{m_W}{\sqrt{s}} \exp(Y)$$

Compared with the dependence on μ_{split} the scale uncertainty associated with flavour matching is small!

DPD luminosities in the massive scheme: Matching scale dependence.

Finally consider the dependence of LO DPD luminosities for dijet production on the flavour matching scales (at LO, varied by a factor of 2):

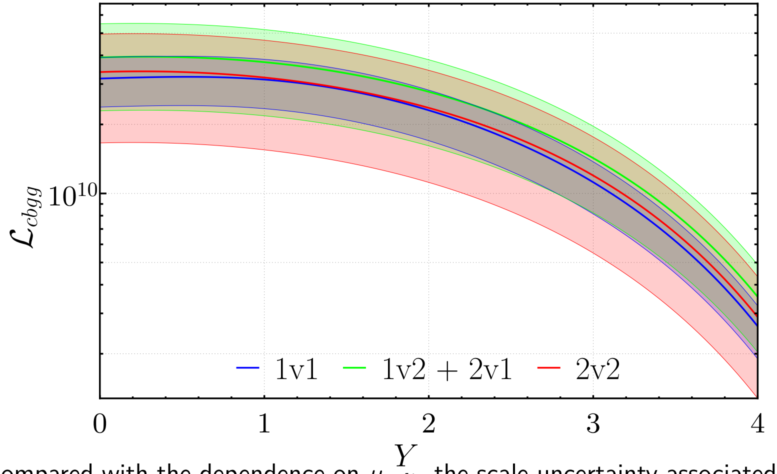

$$x_{1a} = \frac{m_W}{\sqrt{s}} \exp(Y)$$

$$x_{2a} = \frac{m_W}{\sqrt{s}} \exp(-Y)$$

$$x_{1b} = \frac{m_W}{\sqrt{s}} \exp(-Y)$$

$$x_{2b} = \frac{m_W}{\sqrt{s}} \exp(Y)$$

Compared with the dependence on μ_{split} the scale uncertainty associated with flavour matching is small!

Quark mass effects in the $1 \to 2$ splitting.

$\overset{(-)}{q}$